

SANDIA REPORT

SAND98-2702

Unlimited Release

Printed August 1999

Posttest Metallurgical Evaluation Results for Steel Containment Vessel (SCV) High Pressure Test

J. A. Van Den Avyle
K. H. Eckelmeyer

Prepared by
Sandia National Laboratories
Albuquerque, New Mexico 87185 and Livermore, California 94550

Sandia is a multiprogram laboratory operated by Sandia Corporation,
a Lockheed Martin Company, for the United States Department of
Energy under Contract DE-AC04-94AL85000.

Approved for public release; further dissemination unlimited.

Prepared for



Nuclear Power Engineering Corporation



Nuclear Regulatory Commission

Issued by Sandia National Laboratories, operated for the United States Department of Energy by Sandia Corporation.

NOTICE: This report was prepared as an account of work sponsored by an agency of the United States Government. Neither the United States Government, nor any agency thereof, nor any of their employees, nor any of their contractors, subcontractors, or their employees, make any warranty, express or implied, or assume any legal liability or responsibility for the accuracy, completeness, or usefulness of any information, apparatus, product, or process disclosed, or represent that its use would not infringe privately owned rights. Reference herein to any specific commercial product, process, or service by trade name, trademark, manufacturer, or otherwise, does not necessarily constitute or imply its endorsement, recommendation, or favoring by the United States Government, any agency thereof, or any of their contractors or subcontractors. The views and opinions expressed herein do not necessarily state or reflect those of the United States Government, any agency thereof, or any of their contractors.



Posttest Metallurgical Evaluation Results for Steel Containment Vessel (SCV) High Pressure Test

J. A. Van Den Avyle
Materials Processing Department

K. H. Eckelmeyer
Microstructural Analysis Department

Sandia National Laboratories
P.O. Box 5800
Albuquerque, NM 87185

Abstract

The Nuclear Power Engineering Corporation (NUPEC) of Japan and the US Nuclear Regulatory Commission (NRC), Office of Nuclear Regulatory Research, are co-sponsoring and jointly funding a Cooperative Containment Research Program at Sandia National Laboratories. As a part of this program, a steel containment vessel (SCV) model was tested to failure in the high pressure test on December 11–12, 1996. The model, which is representative of a steel containment for an improved Japanese Mark II Boiling Water Reactor Plant, has a geometric scale of 1:10 and a thickness scale of 1:4. The objectives of the SCV model test were to obtain measurement data of the structural response of the model up to its failure in order to validate analytical modeling, to find the pressure capacity of the model, and to observe the failure mechanisms.

The SCV model was nitrogen pressure tested until leaking was detected. Deformation in the model produced different types of damage at several locations. Damage included tears, localized plastic deformation and necking, and general plastic strain. This report examines each damage site to determine the damage mechanisms and to assess whether factors such as alloy properties, assembly procedures, or pre-existing flaws could have contributed to the observed features.

Damage locations on the interior and exterior walls of the model were visually inspected and photographed. Pieces containing damage sites were cut out of the model wall; these were further sectioned for metallurgical analysis, which included optical microscopy, hardness tests, and fracture surface observations.

Tears produced in the model wall adjacent to the equipment hatch and at the opening in the middle stiffener ring were the result of local plastic deformation and ductile shear fracture. At

similar symmetrical locations in the structure, local necking without tearing was also observed. No contributing flaws in the model wall were noted at these locations.

Two types of steel microstructures were found: one typical of a ferritic and pearlitic hot-rolled steel, and one characteristic of a higher hardness low-carbon martensitic/bainitic steel (presumably specified for more highly stressed areas). Heat from the welding process of the SCV model resulted in localized microstructural alteration and reduced hardness and strength in the martensitic/bainitic steel. When the model was pressurized, plastic deformation occurred preferentially in these softer areas, eventually resulting in shear failure adjacent to the weld.

INTENTIONALLY LEFT BLANK

Contents

1. Introduction.....	9
2. Description of SCV Model	9
3. Description of Damage and Sample Locations.....	9
3.1 Tear and Deformation at the Equipment Hatch (EQH)	13
3.2 Tearing and Deformation at Openings in the MST Ring	13
3.3 Localized Deformation at Vertical Welds in LCS Segment	16
4. Steel Alloy Microstructures and Properties	18
4.1 Alloy SGV480	18
4.2 Alloy SPV490	19
4.3 Weld Metal	20
5. Metallographic Analysis of Damaged Regions	26
5.1 Samples from Damaged Region around EQH	26
5.2 Samples from Damaged Region at Ring Stiffener/Wall Area	28
5.3 Samples from Deformed Vertical Weld Area.....	35
6. Conclusions.....	35
7. References.....	36
Appendix A Material Property Data and Inspection Certificates.....	A-1
Appendix B All Sample Hardness Measurements (Rockwell B Scale).....	B-1

Figures

2-1. SCV model elevations and material thickness.	10
2-2. Elevation view of SCV model wall showing sampling locations.....	10
3-1. Exterior view of the equipment hatch (after removal of the barrel) showing torn and necked locations.....	12
3-2. Interior view of wall tear in vertical weld below opening in MST stiffener. Dark material is residue of putty used to seal opening area for post-test leak test.	12
3-3. Overall external view of necked vertical weld in LCS model section	14
3-4. External view of EQH showing tear at 74° and sample locations (Ruler marking in inches).....	14

3-5. Interior view of tear at 74° location near the EQH.....	15
3-6. External view of EQH showing necked region at 106° and sample locations (ruler markings in inches).	15
3-7. Internal view of EQH showing necked region at 106° with displacements.	16
3-8. External view of tear below MST ring at 201°.	16
3-9. Closeup of exterior view of local deformation (causing cracks in paint) at the vertical weld in LCS at 340°. ..	17
3-10. Sample SCV-340 taken from vertical weld in LCS at 340° (external view).....	17
4-1. Banded ferrite and pearlite microstructure typical of SGV480 base metal, 400×.....	22
4-2. Banded ferrite and pearlite microstructure typical of SGV480 heat affected zone, 400×.....	22
4-3. Widmanstatten ferrite and pearlite microstructure seen in hottest regions of SGV480 heat affected zone, 400×.	23
4-4. Low-carbon martensite or bainite microstructure typical of SPV490 base metal, 400×.....	23
4-5. Banded microstructure typical of SPV490 heat affected zone, 100×.....	24
4-6. Ferrite and pearlite microstructure typical of SPV490 heat affected zone, 400×.....	24
4-7. Widmanstatten ferrite or low-carbon martensite/bainite microstructure seen in some areas of SPV490 heat affected zone, 400×.	25
4-8. Widmanstatten ferrite and pearlite microstructure typical of last pass fusion zones in all samples, 100×.....	25
4-9. Equiaxed ferrite and pearlite microstructure typical of fusion zones altered by subsequent weld passes, 400×.	26
5-1. Sample SCV-74-1 near bottom of tear adjacent to EQH, 5×; (a) shear tear in lower hardness weld HAZ in 9 mm SPV490 wall material, with weld fusion zone on right; (b) view to right of (a) showing fusion zone and weld HAZ into 17.5 mm SPV490 reinforcement plate. Reaustenitized HAZ areas are dark regions on either side of fusion zone.	29
5-2. Sample SCV-74-3 near top of tear adjacent to EQH, 5×; (a) deformed and necked region in weld HAZ of 8.5 mm SGV480 wall material with weld fusion zone on right; (b) view to right of (a) showing fusion zone and weld HAZ into 17.5 mm SPV490 reinforcement plate.	30
5-3. Microstructure of necked region at 106° location near EQH, sample SCV-106-1, 5×; (a) thinning deformation in weld HAZ in SPV490 alloy plate with weld fusion zone at right side; (b) view to right of (a) showing weld fusion zone and HAZ of 17.5 mm SPV490 reinforcement plate.	31
5-4. Microstructure of necked region at 106° location near EQH, sample SCV-106-2, 5×; (a) thinning deformation at base metal and weld HAZ in SPV490 alloy plate with weld fusion zone at right side; (b) view to right of (a) showing weld fusion zone and HAZ of 17.5 mm SPV490 reinforcement plate.	32
5-5. Local shearing associated in Sample SCV-74-2 with tearing near inner and outer surfaces near tear initiation site, and typical of the entire tear away from the initiation site, 100×.	33
5-6. Relative absence of local shearing below the fracture surface in the interior of Sample SCV-74-2 denotes the actual fracture initiation site, 100×.	33
5-7. SEM image of ductile shear fracture on tear surface of SCV-74-2 sample taken from tear near EQH (round balls are surface contaminates on the sample).	34
5-8. Microstructure of Sample SCV-21. The neck in the vessel wall is located at the left side of the bottom of the hole in this view.	34
5-9. SEM image of ductile shear fracture on tear surface of SCV-201 sample taken from tear in wall below stiffener.	35
5-10. Cross-section microstructure of vertical weld at 340° between plates of 9 mm SPV490 steel, Sample SCV-340; (a) plate material at left, necked HAZ at center, and weld fusion zone at right; (b) weld area to right of (a) showing, left to right, weld fusion zone, slightly necked HAZ, and 9 mm plate.	37

Tables

4-1. SCV Steel Alloy Compositions and Properties from Inspection Certificates (Mechanical Properties: Transverse to the Rolling Direction)	19
4-2. Hardness Values for SCV Samples	21
5-1. Thickness Reduction Measured in Necked Regions of Each Sample	27

INTENTIONALLY LEFT BLANK

1. Introduction

This report details the results of a visual and metallurgical analysis of the steel containment vessel (SCV) model after the high pressure test which caused damage at several locations on the model. The high pressure test was performed December 11–12, 1996. During the test, dry nitrogen gas at ambient temperature was pumped into the model to a maximum pressure of 4.66 MPa, when leaking was noted. The test lasted approximately 16.5 hours. The purpose of this analysis is to determine the extent that the condition and properties (such as microstructure, strength, ductility, or flaws) of the two steels, SGV480 and SPV490, and assembly features contributed to the damage observed at each location. In particular, this analysis attempts to assess whether the damage was “premature,” resulting from existing properties of the steels. Findings from this report should be evaluated in conjunction with the results of the posttest model analysis in order to complete a comprehensive failure analysis of the model.

2. Description of SCV Model

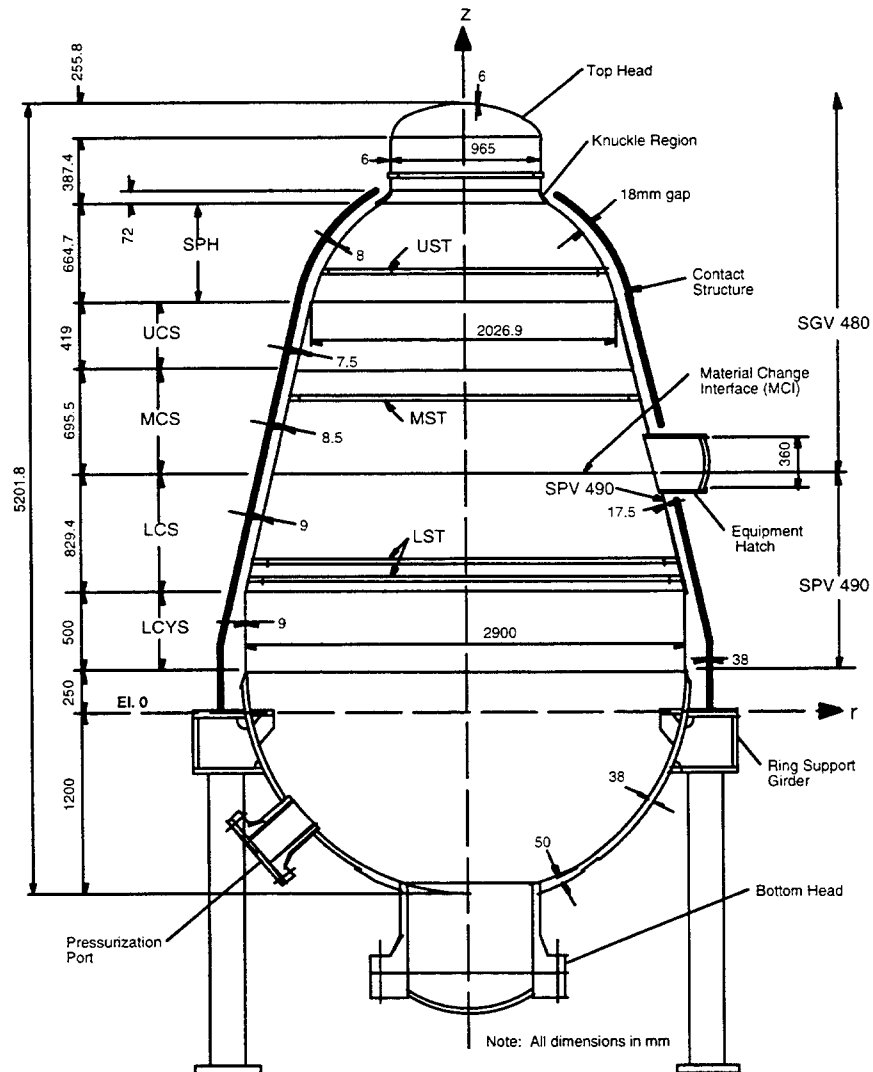
The SCV model is a mixed-scale model, with 1:10 in containment geometry and 1:4 in shell thickness from a prototype Improved Mark II Boiling Water Reactor (BWR) containment structure, of a reactor containment vessel constructed of welded steel plate of several thicknesses (Figure 2-1). Wall thicknesses vary from 6 to 9 mm in the top two-thirds of the structure; the bottom hemisphere is much thicker (38–50 mm). During the test, the upper portion of the vessel was surrounded by a 38-mm-thick contact structure which limited the outward expansion of the SCV model as the pressure increased. The contact structure was removed after the test to permit observations of the outside surface of the model. An equipment hatch (EQH) is built into the side of the model at approximately 2.9 m up from the bottom; it is welded into a ring of thicker (17.5 mm) alloy. The structure also contains internal circumferential stiffener rings at four vertical locations.

An “unrolled” 360° elevation view of the model wall from the outside is shown in Figure 2-2; the area shown extends from the top of the bottom hemisphere to the top of the model. Positions along the circumference are given in degrees (e.g., the equipment hatch is located at the 90° location). Figure 2-2 also shows the stiffener ring positions.

3. Description of Damage and Sample Locations

Three types of localized damage regions were observed on the model. These are discussed in detail in following sections of this report. Damage locations and approximate sizes of sections cut from the model are given in Figure 2-2.

1. At the equipment hatch, a tear formed at the 74° azimuth at the junction of the hatch reinforcement plate and the 9 mm lower conical shell section (LCS) plate material. Symmetrically on the other side of the hatch at the 106° location, a localized neck formed at the similar position (Figure 3-1).
2. Damage occurred at two locations 180° apart, associated with the middle stiffener (MST) ring. A tear formed in the model wall below a weld relief hole in the stiffener ring (Figure 3-2) at position 201°, and a local neck formed in the similar location at 21°.



Nomenclature:

Location Designation

THD
KNU
SPH
UST
UCS
MST
MCS
MCI
LCS
LST
LCYS

Description

top head
knuckle
spherical shell
upper stiffener
upper conical shell
middle stiffener
middle conical shell
material change interface
lower conical shell
lower stiffeners
lower cylindrical shell

Figure 2-1. SCV model elevations and material thickness.

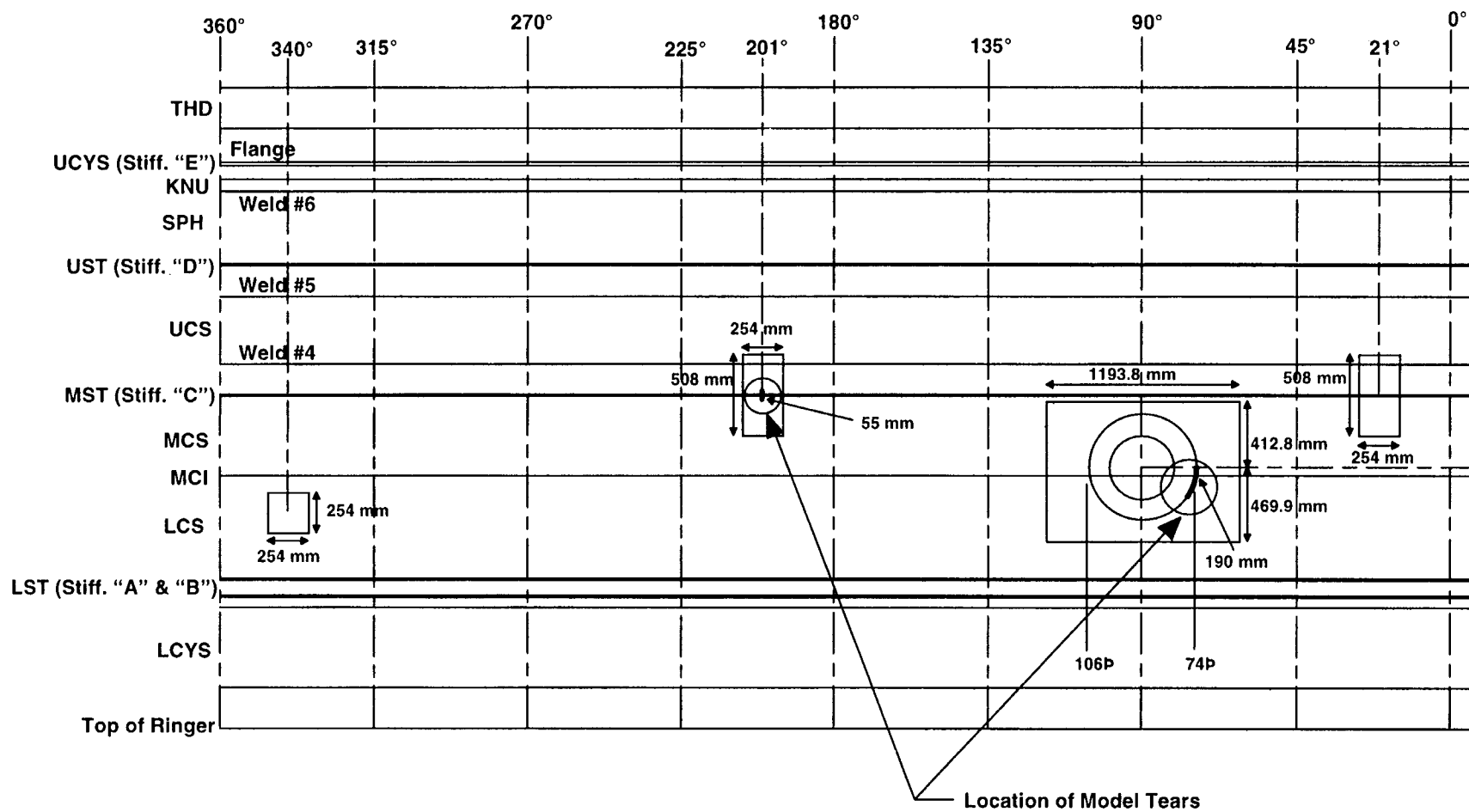


Figure 2-2. Elevation view of SCV model wall showing sampling locations.

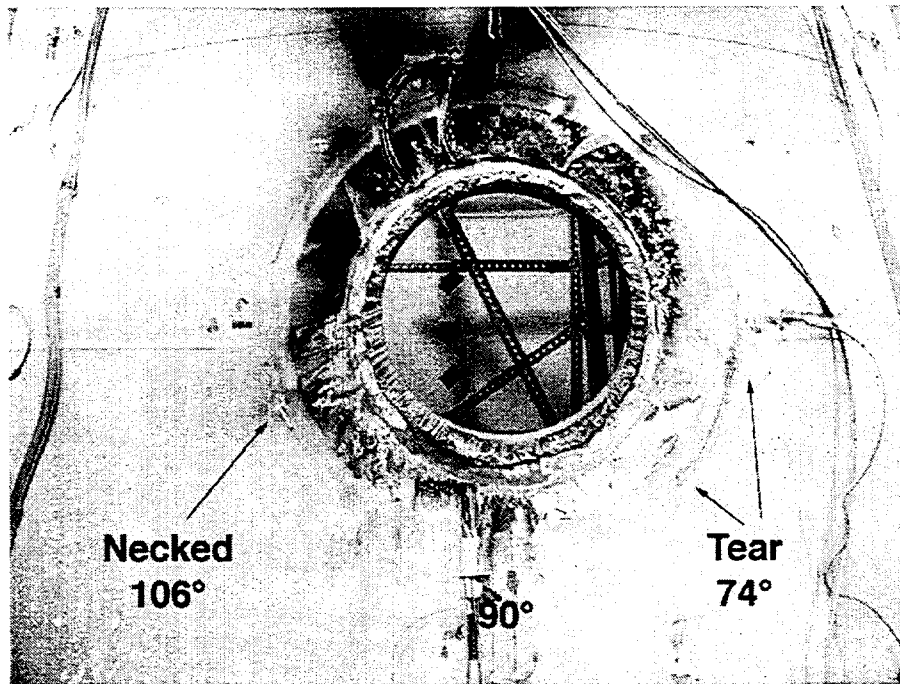


Figure 3-1. Exterior view of the equipment hatch (after removal of the barrel) showing torn and necked locations.



Figure 3-2. Interior view of wall tear in vertical weld below opening in MST stiffener. Dark material is residue of putty used to seal opening area for posttest leak test.

3. Local necks formed within the vertical weld lines at the 160° and 340° positions which connect the two plates forming the LCS (Figure 3-3). These necks and other areas of local deformation on the outer surface of the model are visible because the paint coating is brittle and cracks.

3.1 Tear and Deformation at the Equipment Hatch (EQH)

The tear at the 74° position near the equipment hatch was approximately 190 mm long, with an additional several centimeters of localized necking extending from either end of the tear (Figure 3-4). The local deformation is evident from the cracked paint. An interior view of the same tear is shown in Figure 3-5; note the position of strain gages near the tear. Three samples were cut from the area of the tear for metallurgical analysis. These included SCV-74-1 and SCV-74-3, which came from the untorn locally deformed regions on either end of the tear, and were mounted and sectioned to examine the deformation and local microstructures. Sample SCV-74-2 spanned the tear, and its fracture surfaces were analyzed by scanning electron microscopy to determine failure mode.

The structurally equivalent location near the EQH at 106° showed similar localized necking deformation, however here the strain was not large enough to result in tearing (Figure 3-6). The total length of the local deformation was approximately 85 mm. On the interior, the deformation shows up as offsets in ink grid markings in the necked location (Figure 3-7). Two samples, SCV-106-1 and SCV-106-2, were cut from the necked region.

In both of these locations the high strain concentration followed the weld between the thick (17.5 mm) EQH reinforcement plate and the thinner steel plate of the vessel wall. In Figure 3-4 the horizontal measuring tape follows along the material change interface (MCI) along the line of the horizontal weld between model segments LCS (9-mm-thick SPV490 steel) and MCS (8.5-mm-thick SGV480 steel). The reinforcement plate is also SPV490 steel. The majority of the deformation and tearing occurred along the weld between the reinforcement plate and the lower LCS segment; however, the localized strain also followed across the horizontal weld into the thinner MCS material. Sample SCV-74-3 contained material from both alloys (the reinforcement plate and the MCS).

3.2 Tearing and Deformation at Openings in the MST Ring

The MST ring (19 mm thick, 55 mm wide) is welded circumferentially edge-on around the MCS vessel wall segment (8.5-mm-thick SGV480 steel). At locations 21° and 201°, 180° apart, there are semi-circular openings cut out of the stiffener next to the vessel wall to accommodate the vertical welds joining the steel plates forming the MCS. These holes are approximately 32 mm wide. A tear formed in the model wall at the weld relief opening in the stiffener ring at position 201°, and a local neck formed in the similar location at 21°. The tear and local necks are vertically oriented within the vertical weld. Figure 3-8 shows an external view of the torn area at 201°. The figure also shows sample SCV-201 which was cut out transverse to the tear direction; a similar sample was taken at location 21° (SCV-21).

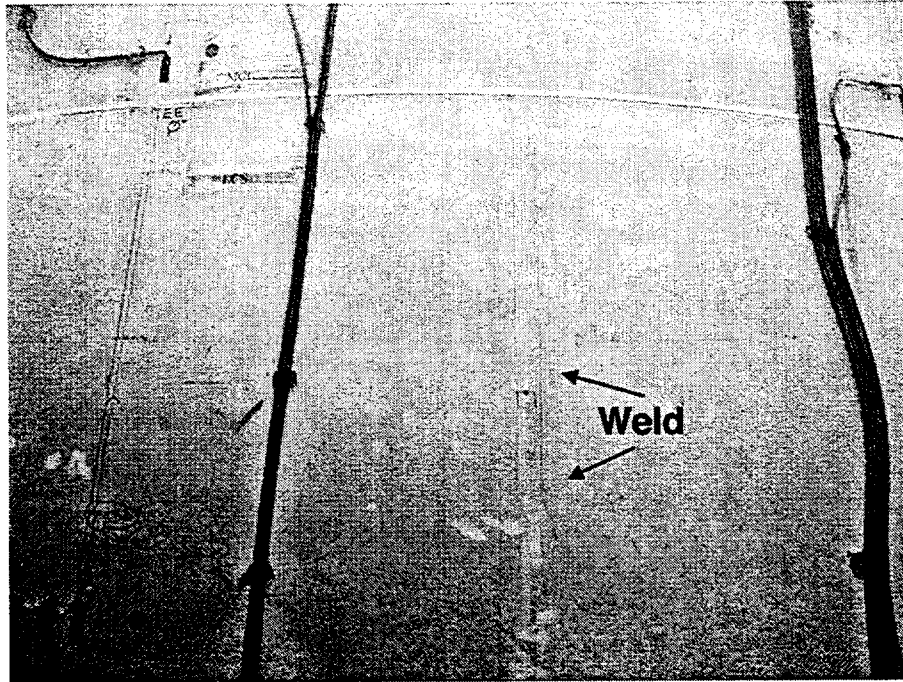


Figure 3-3. Overall external view of necked vertical weld in LCS model section.

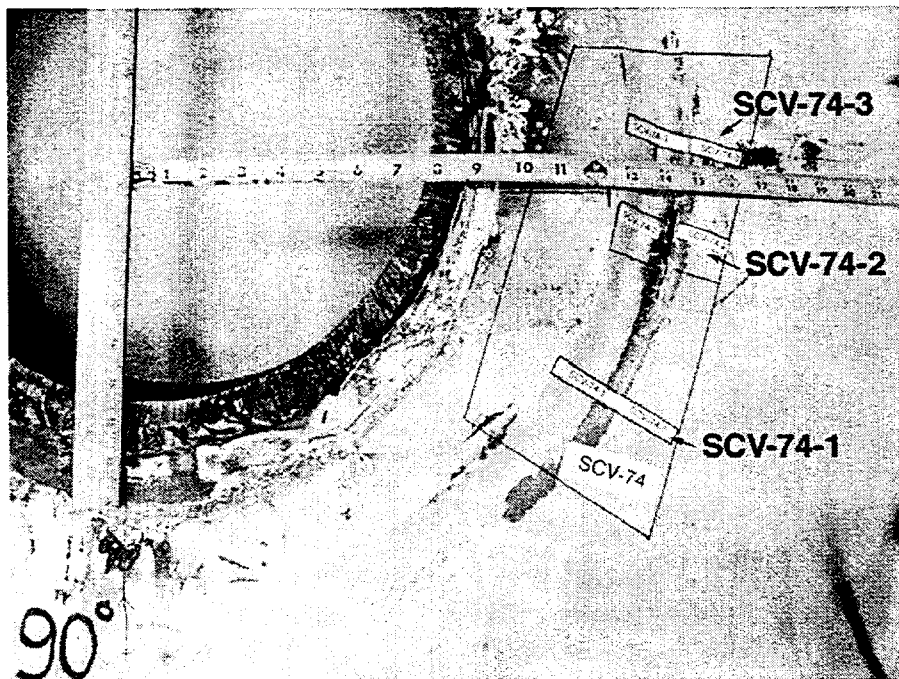


Figure 3-4. External view of EQH showing tear at 74° and sample locations (ruler marking in inches).

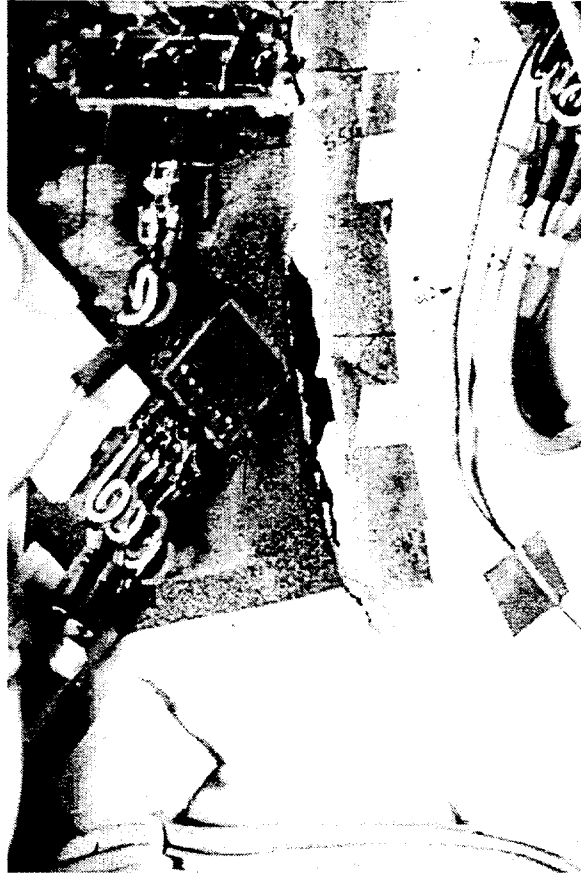


Figure 3-5. Interior view of tear at 74° location near the EQH.

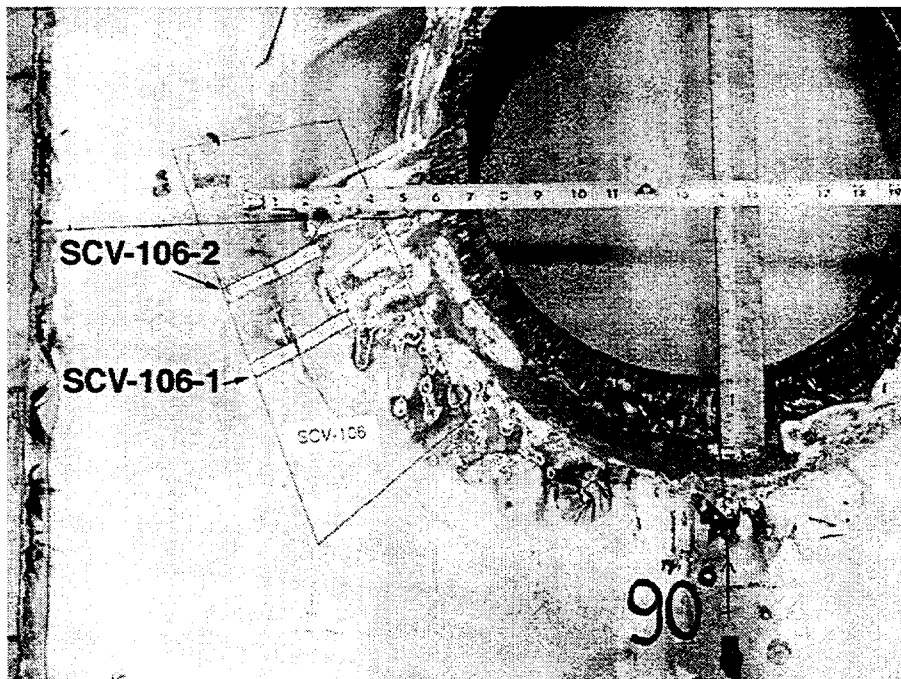


Figure 3-6. External view of EQH showing necked region at 106° and sample locations (ruler markings in inches).

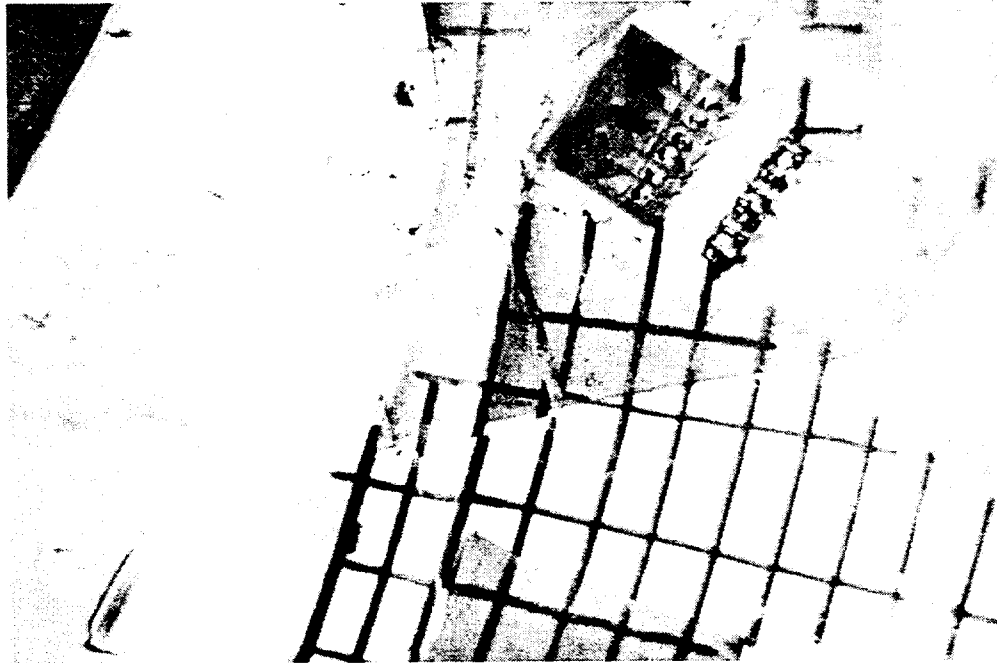


Figure 3-7. Internal view of EQH showing necked region at 106° with displacements.

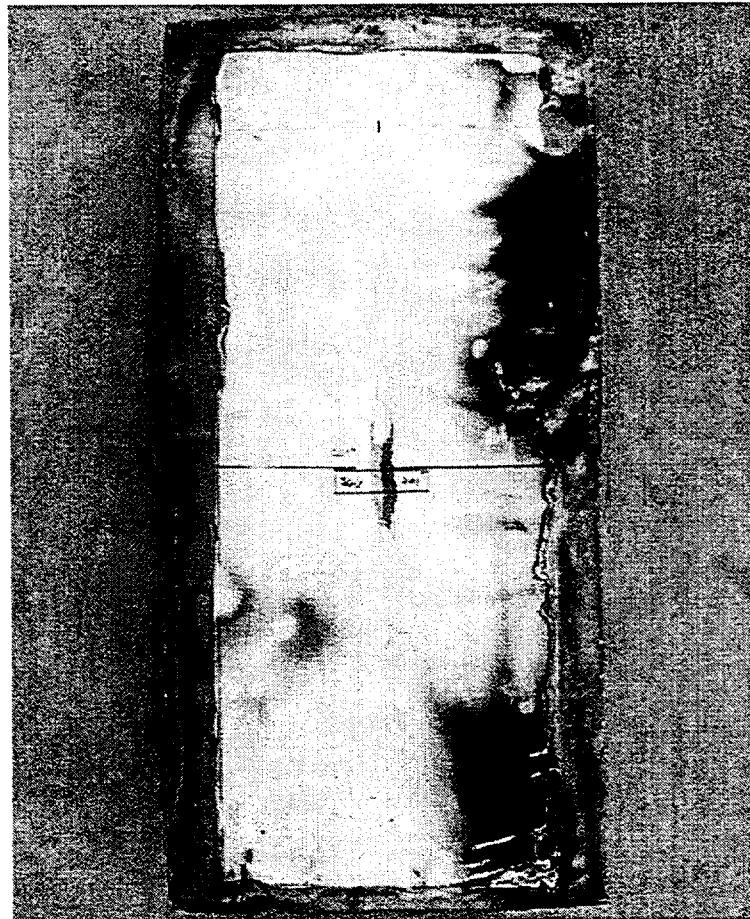


Figure 3-8. External view of tear below MST ring at 201° .

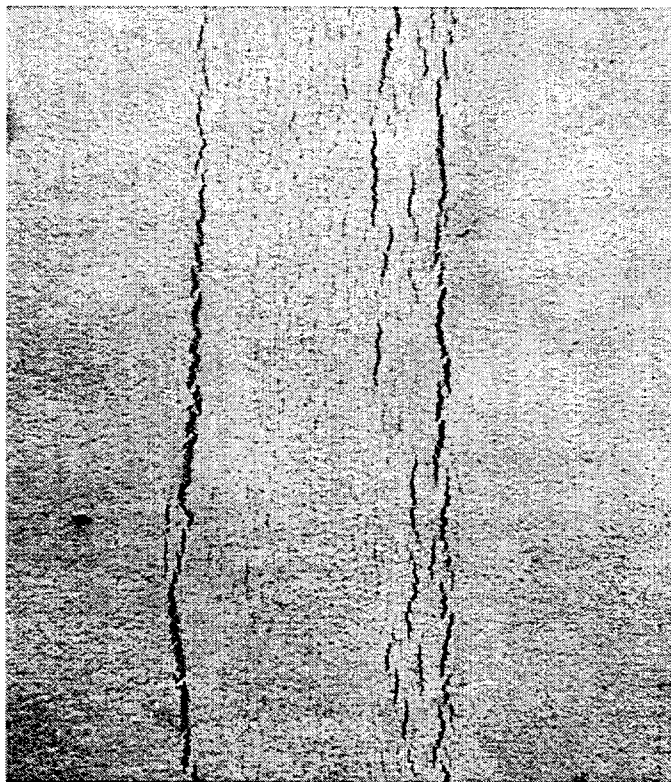


Figure 3-9. Closeup of exterior view of local deformation (causing cracks in paint) at the vertical weld in LCS at 340°.

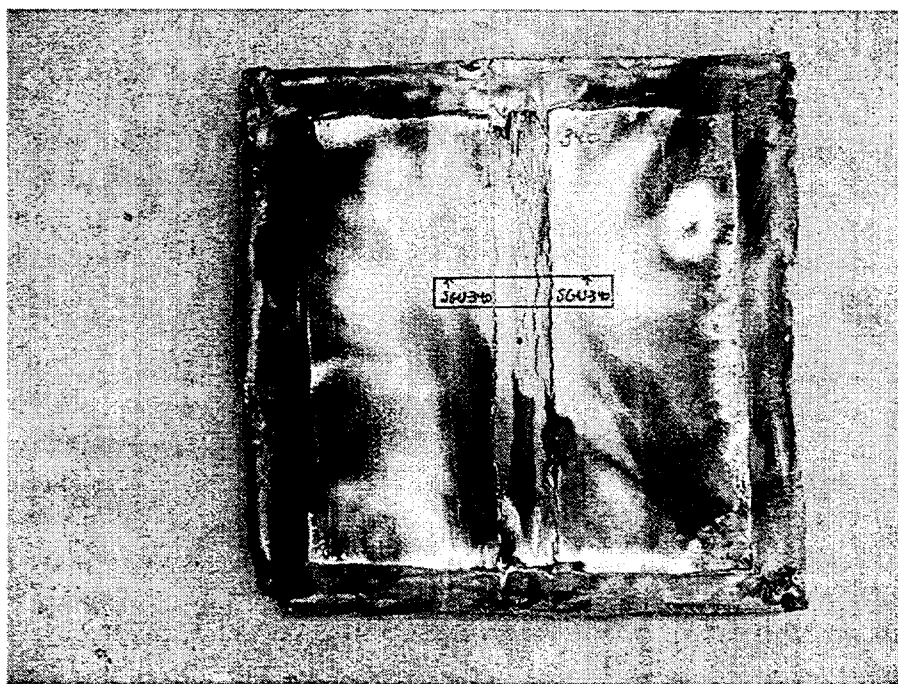


Figure 3-10. Sample SCV-340 taken from vertical weld in LCS at 340° (external view).

3.3 Localized Deformation at Vertical Welds in LCS Segment

Local necks formed within the vertical welds at the 160° and 340° positions which connect the two plates forming the LCS (Figure 3-3). These plates are 9-mm-thick SPV490 steel. A closeup external view of this deformation is given in Figure 3-9. A sample, SCV-340 was cut out for analysis (Figure 3-10).

4. Steel Alloy Microstructures and Properties

Table 4-1 gives reported compositions, strength, and ductility values for several thicknesses of the two alloys used to construct the model. These were taken from the material inspection certificates (see Appendix A). Analysis of polished cross-sections of the above samples showed that the two alloy steels were substantially different.

To characterize the relative strength levels of welds and alloy base metal at regions of the steel containment vessel (SCV) model where damage occurred, indentation hardness measurements were taken on the samples cut for metallurgical analysis. All hardness measurements, which used the Rockwell B scale, were calibrated to standard test blocks, and were taken in the thickness dimension of the steel plates. Sample surfaces were ground and polished. Hardness values were correlated to ultimate tensile strength using published tables for carbon steel (*ASM Metals Handbook*, 1967). Base metal hardness measurements were typically taken at the edge of the cut specimen, as far as possible from any weld within the sample. Base metal hardness would normally refer to metal plate which did not experience plastic deformation or any weld heating. In some cases, however, the “base metal” location may have experienced some heating from the weld process, and in all cases the “base metal” hardness was likely influenced by overall plastic strain in the SCV model wall.

4.1 Alloy SGV480

This material was found in sample SCV-21 and the thinner half of sample SCV-74-3. From its inspection certificates, it was specified to have 265 MPa minimum yield strength, 480 to 590 MPa ultimate tensile strength (UTS), and a minimum elongation of 15–17%, depending on thickness. The data shown in Table 4-1 and Appendix A indicate the material met these specifications.

This alloy’s base metal microstructure was found to consist of a heavily banded ferrite and pearlite (Figure 4-1). This is typical of hot-rolled carbon steel. Its hardness was found to be 89.2 Rockwell B, suggesting an UTS of ~610 MPa (*ASM Metals Handbook*, 1967). Average hardness measurements are given in Table 4-2; a complete listing of all hardness values is given in Appendix B. This is ~10% higher than the reported UTS of 560 MPa, indicating that this material experienced net section yielding and a small amount of plastic deformation strain hardening during testing of the model. No undeformed material was available for hardness testing, since the SCV model experienced plastic deformation.

When welded, the reaustenitized heat affected zone (HAZ) transformed mostly to a ferrite and pearlite microstructure similar to, but somewhat finer than the base metal (Figure 4-2). Some

**Table 4-1 SCV Steel Alloy Compositions and Properties from Inspection Certificates
(Mechanical Properties: Transverse to the Rolling Direction)**

Alloy	Thickness (mm)	Composition (%)	Yield Strength (MPa)	Tensile Strength (MPa)	Elongation (%)
SGV480	7.5	0.18 C, 0.23 Si, 1.16 Mn, 0.007 P, 0.001 S	403	556	26
SGV480	8	Same as above	389	532	26
SGV480	8.5	Same as above	411	560	24
SPV490	9	0.10 C, 0.24 Si, 1.29 Mn, 0.002 P, 0.001 S, 0.48 Ni, 0.03 Cr, 0.17 Mo, 0.04 V	710	727	27
SPV490	38	Same as above	566	650	45

portions immediately adjacent to the weld and near the surface (where very high temperatures resulted in very large austenite grains) transformed to a microstructure of Widmanstatten ferrite and pearlite (Figure 4-3). The Widmanstatten structure is a fine needle-like microstructure, as opposed to equiaxed grains of mixed ferrite and pearlite (compare Figures 4-3 and 4-9). It is a geometric microstructure that results from formation of a new phase along certain crystallographic planes of the parent solid solution phase. The Widmanstatten structure can form in many alloys with certain heat treatments or cooling rates. A few hardness measurements indicated that the heat affected zone was slightly harder than the base metal, 92.8 Rockwell B, because of its finer microstructure.

Based on the Widmanstatten microstructures, it is unlikely that the properties of this material would change significantly with variations in section thickness.

4.2 Alloy SPV490

This material was found in the thicker half of sample SCV-74-3, as well as in both halves of samples SCV-74-1, SCV-106-1, SCV-106-2, and SCV-340. It was specified to have 490 MPa minimum yield strength, 610 to 740 MPa ultimate tensile strength, and 18-25% elongation. Reported measured yield and ultimate tensile strengths (UTS) were 710 and 727 MPa, respectively, for the 9 mm plate material (Table 4-1). Strengths were substantially lower for the 38 mm material (566 and 650 MPa).

Base metal hardness measurements from an as-received reference plate of SPV490, which is not a part of the model, showed an average Rockwell B value of 98.8 ± 0.7 (Table 4-2). This compares to an overall average base metal hardness from the cut samples of 97.4 Rockwell B, correlating to a UTS of ~733 MPa. This is consistent with the reported UTS of 727 MPa.

This alloy was found to have a much different microstructure typical of low-carbon martensite or bainite (Figure 4-4). This was most likely obtained by accelerated cooling from the hot rolling (or austenitizing) temperature (*ASM Metals Handbook*, 1990). SPV490 is clearly a more sophisticated steel than SGV480. This steel's higher strength is very likely due to the presence of carbon in solid solution or as finely divided carbides in the martensite or bainite, as well as finely divided vanadium carbonitrides (none of these is resolvable by optical metallography). Both result from a combination of alloying and a carefully controlled deformation and cooling sequence.

When welded, a much different microstructure develops in the reaustenitized heat affected zone. At 100× this microstructure appears significantly banded, indicating a pattern of chemical segregation that was not apparent in the martensitic/bainitic base metal (Figure 4-5). Higher magnification examination reveals the presence of a small amount of pearlite in the darker etching bands, consistent with 0.1% carbon (Figure 4-6). The remainder of the microstructure appears to consist of ferrite grains. In some areas these are fairly equiaxed, while in others they are more elongated and plate-like, typical of Widmanstätten ferrite or low-carbon martensite/bainite (Figure 4-7).

The heat affected zones (HAZs) were found to have significantly lower hardness, 90.7 Rockwell B in HAZs that had not been substantially deformed (Table 4-2). Measurements of undeformed HAZs were taken on the 17.5-mm-thick plate side of the welds, where the increased thickness did not allow plastic deformation. This suggests a HAZ ultimate tensile strength of ~625 MPa, 100 MPa lower than that of the base metal, and near the lower UTS design specification limit. More detailed hardness measurements indicated that the lowest HAZ hardness occurs near both sides of the boundary of the reaustenitized HAZ and the adjacent partially austenitized material, where the alloy was completely tempered, but not austenitized. These areas of lowest hardness are the logical result of heating causing removal of carbon from solid solution (or very finely divided carbides) through coarsening, as well as coarsening or resolution of fine carbonitride precipitates.

The band of reduced hardness is quite narrow, at least in the thick sections; it is approximately 2 to 3 mm wide in the thick (17.5 mm) sections of SPV490. Beyond that, the hardness seems roughly equivalent to that of the bulk base metal. The present samples do not permit measurement of the width of decreased hardness band in thin SPV490. This is where extensive deformation and necking occurred in the SCV samples.

The metallurgy of this steel, particularly the controlled cooling required to obtain the desired mechanical properties, makes it highly likely that properties would vary with section thickness. This apparently is responsible for the lower strengths reported in Table 4-1 for thicker sections of this material.

4.3 Weld Metal

Metallographic examination revealed that all of the welds were made in multiple passes. Frequently the initial passes were made on the inside of the model and the later passes on the outside. The microstructure of the final fusion zones consisted of large elongated prior-austenite grains in which the grain boundary regions had transformed to ferrite and the grain centers had

transformed to Widmanstätten ferrite and pearlite (Figure 4-8). The underlying prior fusion zones had been altered/transformed during subsequent weld passes, and consisted of much finer equiaxed ferrite grains and pearlite colonies (Figure 4-9). The hardness of the fusion zones (Table 4-2) was found to average Rockwell B 95.6, with the final fusion regions being slightly harder (~97), and the altered earlier passes being slightly softer (~94). No significant weld defects were observed in any of the samples.

Table 4-2. Hardness Values for SCV Samples

Listed in order are: Rockwell B Hardness Averages, Standard Deviations, and Numbers of Measurements

Sample	Material	Base Metal ^a	HAZ	Fusion Zone
SCV-74-1	SPV490	98.1 ±1.03 10	91.5 ±1.06 5	95.1 ±1.05 5
SCV-74-3	SPV490	94.2 ±0.39 5	90.9 ±1.80 5	92.1 ^b ±0.96 5
"	SGV480	89.2 ±0.15 5	92.2 ^c ±1.49 5	Same as above
SCV-106-1	SPV490	97.4 ±1.12 20	92.1 ±1.69 5	97.1 ±1.11 15
SCV-106-2	SPV490	97.0 ±1.34 15	88.6 ±1.04 5	95.0 ±2.58 10
SCV-340	SPV490	98.0 ±0.84 20	96.7 ^c ±1.83 10	97.6 ±0.55 15
SCV-21	SGV480	88.8 ±1.26 5	92.8 ±0.56 4	95.5 ±0.92 6
SGV480 Avg. ^d		89.0	92.8	95.5
SPV490 Avg. ^d		97.4	90.7	96.2
SPV490 Reference Plate	SPV490	98.8 ±0.07 10		

^a "Base Metal" measurements, except for the SPV490 Reference Plate, were taken at the far edges of sectioned samples; these samples experienced some plastic deformation, and the sample edges may have been heated during welding of the structure.

^b Fusion zone between SGV480 and SPV490; not included in averages.

^c HAZ deformed during pressurization of model; it is likely that hardness of material prior to deformation was lower; not included in averages.

^d Weighted averages; more hardnesses measurements were made in some samples than others. See Appendix B.

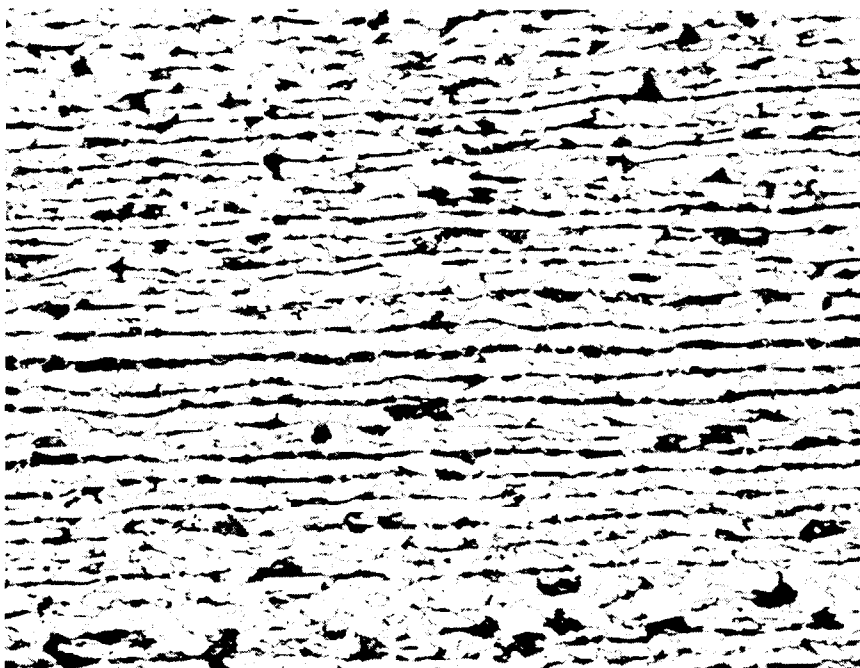


Figure 4-1. Banded ferrite and pearlite microstructure typical of SGV480 base metal, 400 \times .

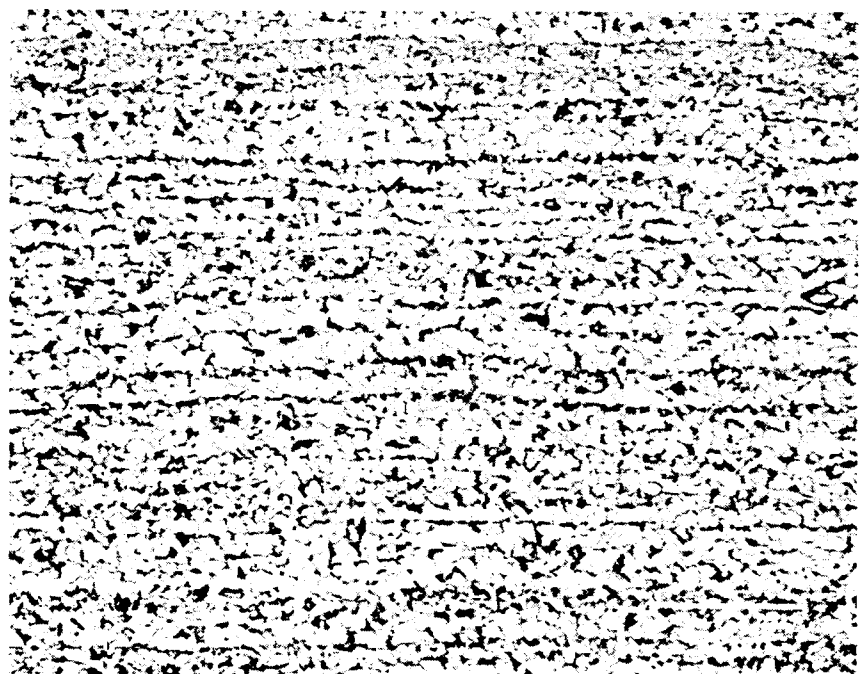


Figure 4-2. Banded ferrite and pearlite microstructure typical of SGV480 heat affected zone, 400 \times .



Figure 4-3. Widmanstatten ferrite and pearlite microstructure seen in hottest regions of SGV480 heat affected zone, 400 \times .

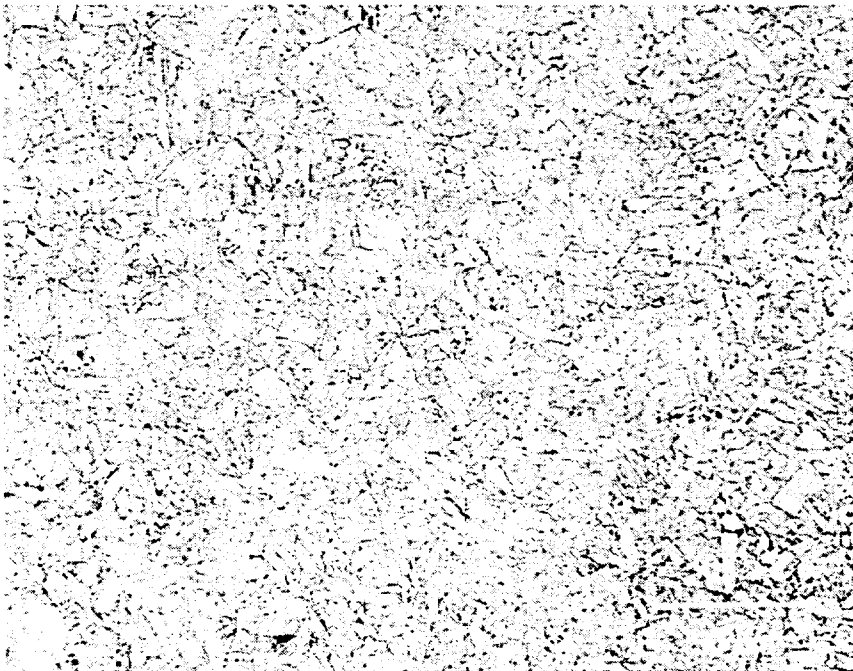


Figure 4-4. Low-carbon martensite or bainite microstructure typical of SPV490 base metal, 400 \times .

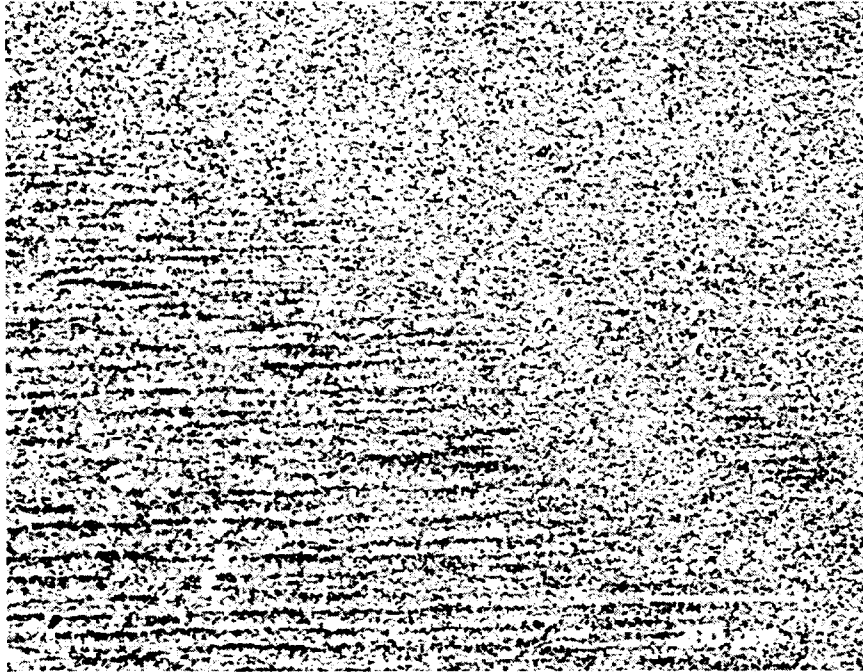


Figure 4-5. Banded microstructure typical of SPV490 heat affected zone, 100×.



Figure 4-6. Ferrite and pearlite microstructure typical of SPV490 heat affected zone, 400×.



Figure 4-7. Widmanstatten ferrite or low-carbon martensite/bainite microstructure seen in some areas of SPV490 heat affected zone, 400 \times .

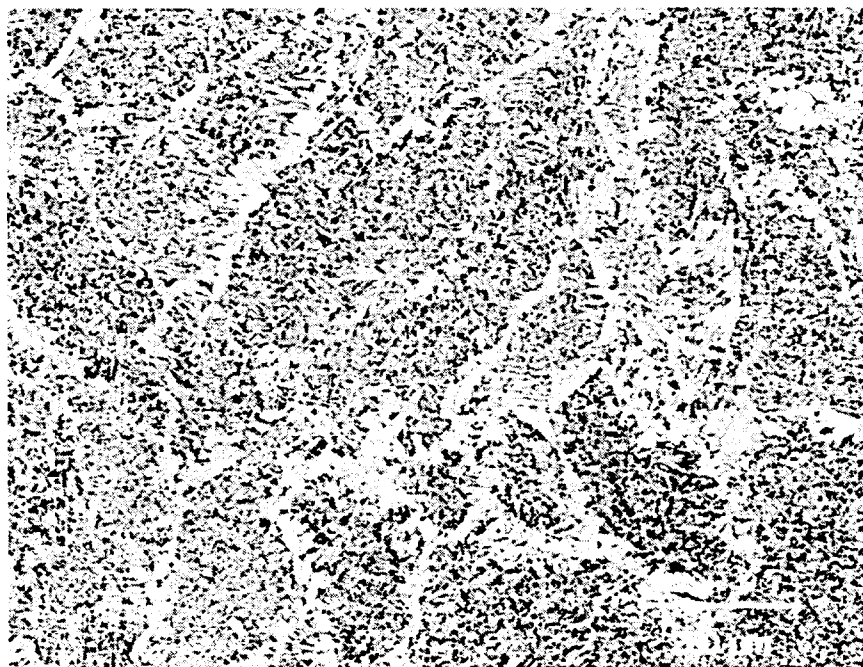


Figure 4-8. Widmanstatten ferrite and pearlite microstructure typical of last pass fusion zones in all samples, 100 \times .

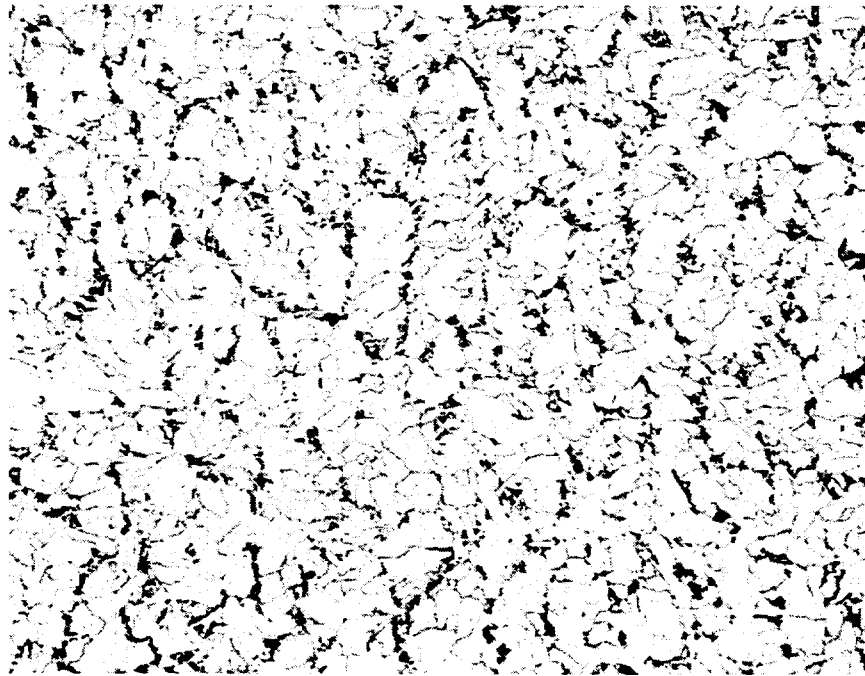


Figure 4-9. Equiaxed ferrite and pearlite microstructure typical of fusion zones altered by subsequent weld passes, 400 \times .

5. Metallographic Analysis of Damaged Regions

5.1 Samples from Damaged Region around EQH

The SCV model test was terminated when a ~190-mm-long tear developed in the wall adjacent to the equipment hatch at the 74° location. Macroexamination of the fracture surfaces indicated that this tear initiated in the 9-mm-thick SPV490 wall near where it was welded to the thicker reinforcement ring of the same material. The tear extended parallel to the weld from this initiation site in both directions, one half remaining in the 9 mm thick SPV490, and the other half crossing into the 8.5-mm-thick SGV480. The corresponding area on the opposite side of the equipment hatch at 106° exhibited substantial necking, but no tearing.

Seven samples were examined from the deformed and torn regions near the EQH: three from the fracture initiation region (SCV-74-2 A, B, and C), one from each end of the tear (SCV-74-1 and SCV-74-3), and two from the necked region on the opposite side of the equipment hatch (SCV-106-1 and SCV-106-2). Each sample consisted of a thin section of the model wall (8.5-mm-thick SGV480 in sample SCV-74-3, or 9-mm-thick SPV490 in all of the other samples) welded to a section of the thicker (17.5 mm) ring of SPV490 that surrounds the equipment hatch. The thickness reductions measured in each of these areas are shown in Table 5-1. It is apparent that both materials underwent substantial plastic deformation prior to tearing.

Metallographic examination of all of these samples revealed weld fusion zones, adjacent weld heat affected zones, and base metal microstructures. These are shown in Figures 5-1 through 5-6.

Table 5-1. Thickness Reduction Measured in Necked Regions of Each Sample

Sample	Material	% Thickness Reduction	Necking and Tear Location
SCV-74-2	SPV490	44.6 ^a	HAZ
SCV-74-1	"	38.4 ^b	HAZ
SCV-74-3	SGV480	41.5 ^b	HAZ
SCV-106-1	SPV490	15.0	HAZ
SCV-106-2	"	31.1	HAZ
SCV-21	SGV480	12.8	HAZ
SCV-201	"	37.8	HAZ
SCV-340	SPV490	11.9 (side 1) 4.2 (side 2)	HAZ

^a Near tear initiation site

^b Just ahead of tear

In all cases necking was found to have concentrated in the weld heat affected zone. Eventual failure occurred by ~45-degree shear in these heavily deformed regions. No other flaws or provocative microstructural features were found to be associated with these failures.

Figure 5-1(a) shows the torn SPV490 HAZ near the lower end of the tear at the 74° location (Sample SCV-74-1). This weld connects the 9 mm SPV490 plate on the left to the 17.5-mm-thick SPV490 reinforcement plate around the EQH. The weld fusion zone, with at least five weld passes, is shown in Figure 5-1(b); the thicker plate is on the right. The necking and subsequent tearing is concentrated approximately 10 mm away from the fusion zone in the lower hardness region of the HAZ. Taken near the other (upper) end of the tear, Sample SCV-74-3 shows a similar view of the necked region in SGV480 plate in the HAZ of the weld to the EQH ring (Figure 5-2). The samples taken from the necked region on the other side (106°) of the EQH have the same appearance (Figures 5-3 and 5-4).

These figures, combined with hardness data discussed in Section 4.2, provide information to estimate the extent of thermal softening of the SPV490 alloy plate away from the welds. The HAZ is comprised of two regions: (1) a dark etching reaustenitized part of the HAZ below the weld fusion zone, etched dark in Figures 5-1 through 5-4, and (2) a lightly etched band of reduced hardness next to the reaustenitized dark HAZ (measured to extend an additional 2 to 3 mm into the thick sections of SPV490). The reaustenitized HAZ depth ranges from 4 to 6 mm for both the thin and thick sides of the welds. This indicates that the depths of thermal penetration were similar for the two thicknesses. Because the band of reduced hardness in the metal adjacent to the reaustenitized portion (dark region) HAZ is approximately 2 to 3 mm wide in the thick

sections of SPV490, it is reasonable to conclude that the reduced hardness band in the thinner plate would also be on the order of 2 to 3 mm.

Metallographic examination of samples near the fracture initiation site (SCV-74-2 A, B, and C) revealed evidence of substantial local plastic shear deformation below the fracture surface near the inner and outer plate surfaces (Figure 5-5), but less local shear deformation in the interior of the model wall (Figure 5-6). *This suggests that failure initiated internally within the material, rather than at surface defects.*

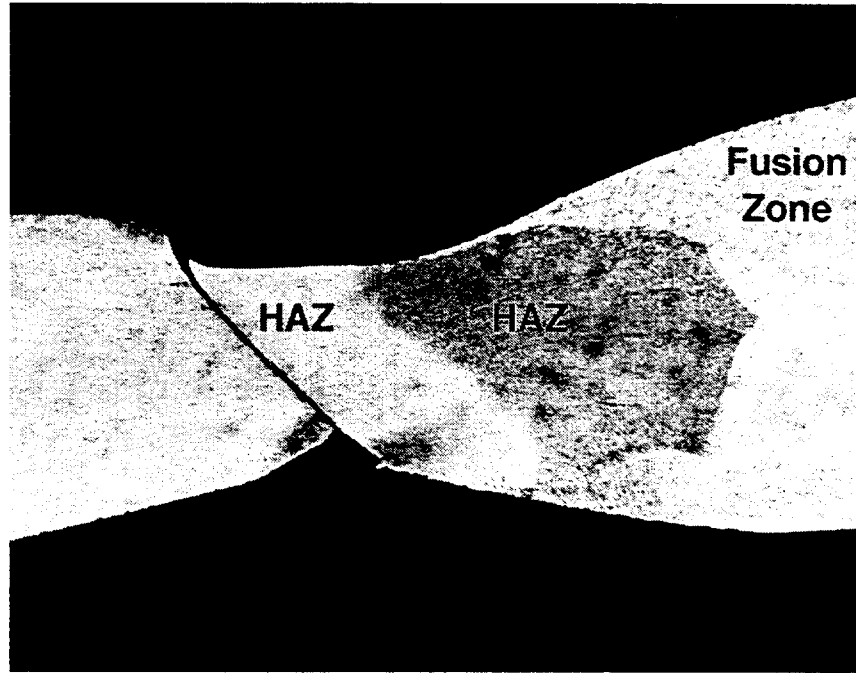
The fracture surface on Sample SCV-74-2 was examined in the scanning electron microscope (SEM) to determine tearing crack growth mode and to check for flaws or initiation sites. *The entire surface of the sample was comprised of ductile shear voids (Figure 5-7) characteristic of ductile shear overload failure.* No surface or subsurface flaws were noted. On these ductile shear void fracture surfaces, it was not possible to locate individual fracture initiation points. The fracture morphology seen here is consistent with ductile overload tearing failure, by shear, after the neck formed.

5.2 Samples from Damaged Region at Ring Stiffener/Wall Area

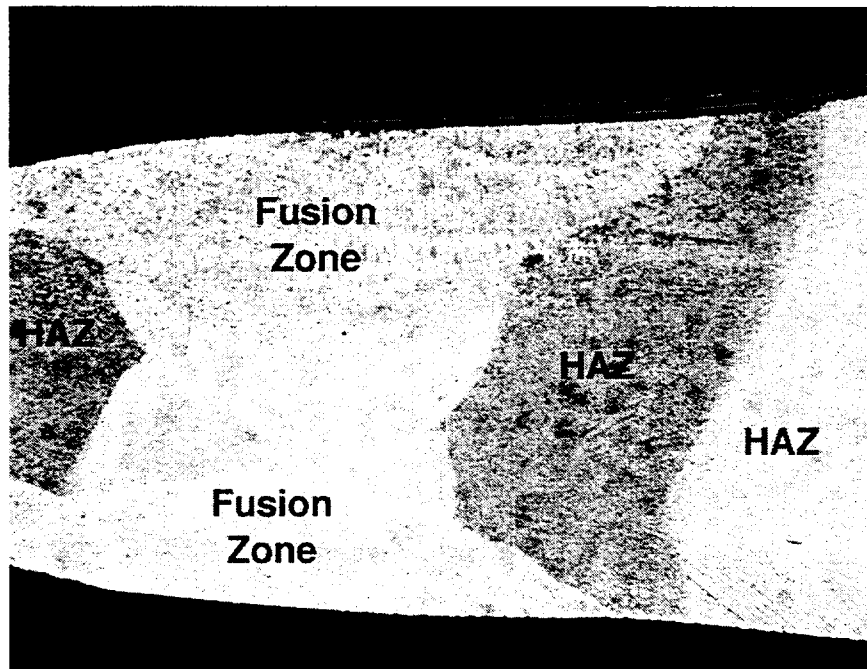
Sample SCV-21 at the 21° location consisted of two sections of 8.5 mm thick SGV480 wall (MCS) vertically welded together and then welded to a perpendicular plate stiffener ring of the same material. This ring was designed with an approximately 32-mm-wide opening adjacent to the inner model surface; the semi-circular openings are over the vertical welds. Deformation of the stiffener ring during pressurization caused localized plastic deformation of the wall at the opening and produced a vertical necked region within the vertical weld.

Sample SCV-21 consisted mostly of weld metal and heat affected zone (Figure 5-8). The sample is aligned along the direction of the stiffener ring, and the opening in the ring is captured in cross-section. The wall plate is at the bottom of the section, with the neck evident at the bottom of the opening (the model vertical direction is perpendicular to the micrograph). A wide variety of microstructures were observed, including the heavily banded ferrite and pearlite base metals, heat affected zones consisting of banded ferrite and pearlite or Widmanstätten ferrite and pearlite (where large austenite grains had formed from very high temperature exposure), decarburized areas where the opening had apparently been flame cut from the stiffener plate, and essentially pure iron weld metal which apparently had been used to build up various surfaces. The necked region is primarily composed of weld HAZ. The hardness of the wall was found to be consistent with that of the SGV480 wall material in sample SCV-74-3. The measured reduction-in-area measured in the wall adjacent to the stiffener cut-out is shown in Table 5-1.

The fracture surface of the tear in Sample SCV-201 was viewed in the SEM to determine the fracture mode (Figure 5-9). This tear formed primarily in shear as a ductile overload failure. The figure shows ductile shear voids on the surface. *No flaws were noted which would have contributed to premature failure.* The measured reduction-in-area measured in the wall adjacent to the stiffener cutout at 201° is shown in Table 5-1.



(a)

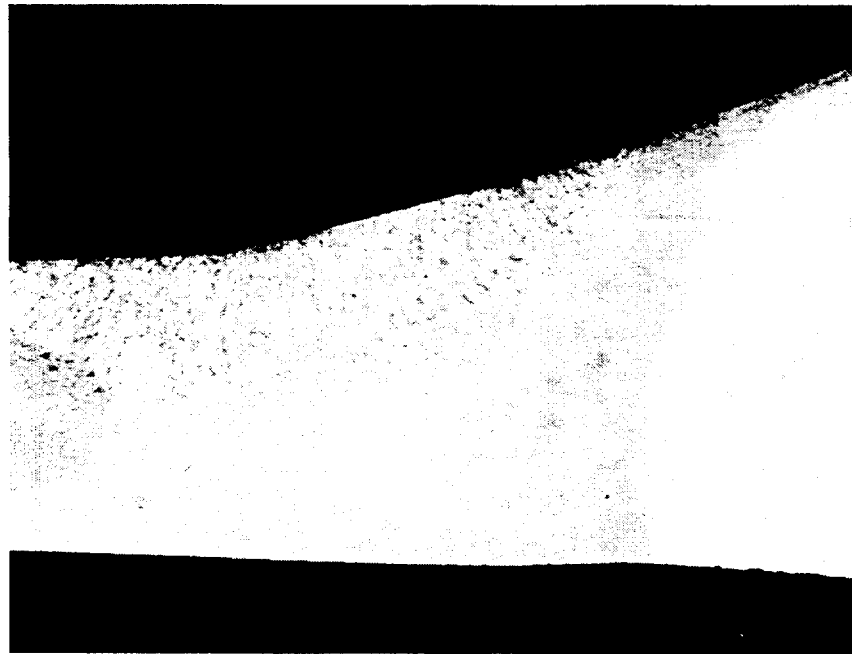


(b)

Figure 5-1. Sample SCV-74-1 near bottom of tear adjacent to EQH, 5 \times ; (a) shear tear in lower hardness weld HAZ in 9 mm SPV490 wall material, with weld fusion zone on right; (b) view to right of (a) showing fusion zone and weld HAZ into 17.5 mm SPV490 reinforcement plate. Reaustenitized HAZ areas are dark regions on either side of fusion zone.

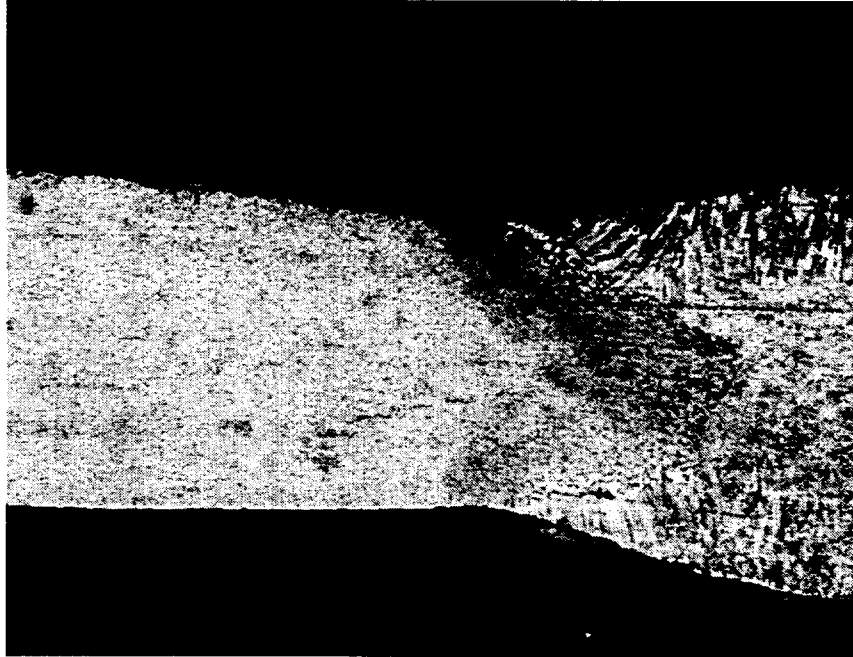


(a)

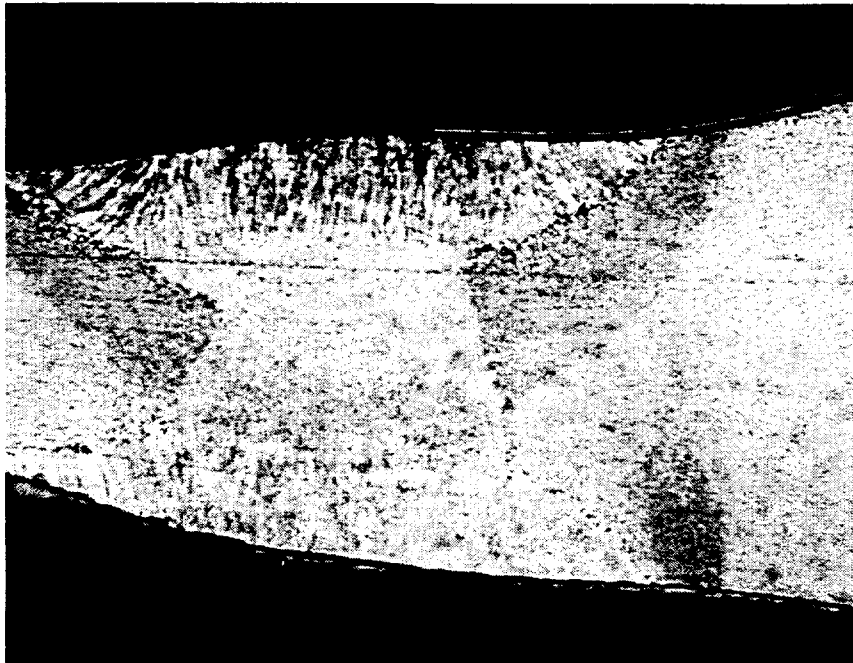


(b)

Figure 5-2. Sample SCV-74-3 near top of tear adjacent to EQH, 5 \times ; (a) deformed and necked region in weld HAZ of 8.5 mm SGV480 wall material with weld fusion zone on right; (b) view to right of (a) showing fusion zone and weld HAZ into 17.5 mm SPV490 reinforcement plate.

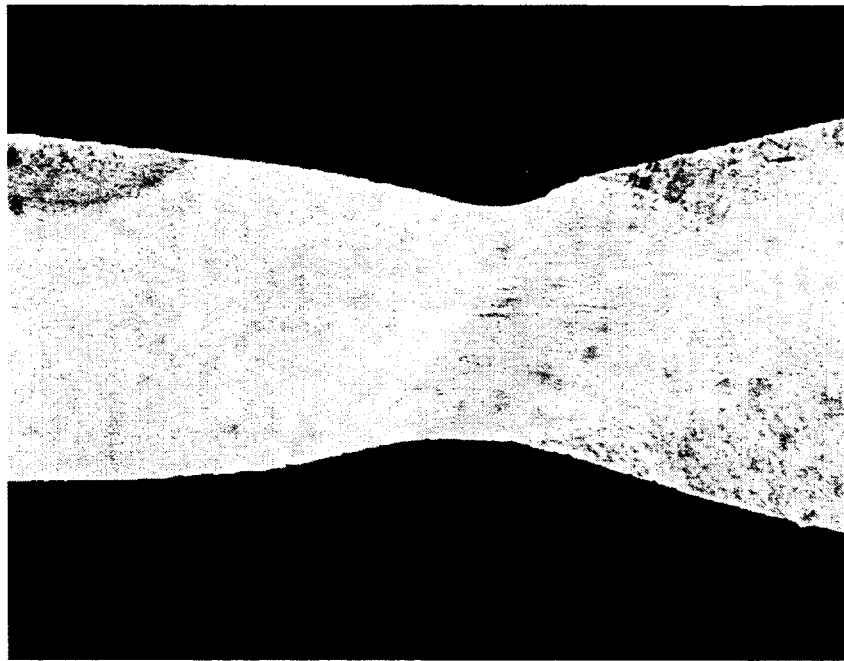


(a)

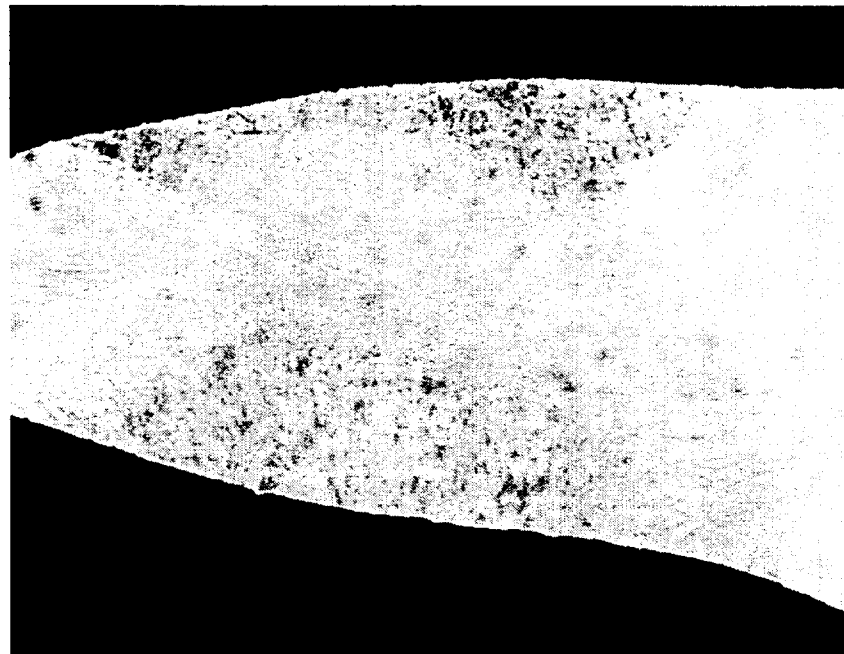


(b)

Figure 5-3. Microstructure of necked region at 106° location near EQH, sample SCV-106-1, 5×; (a) thinning deformation in weld HAZ in SPV490 alloy plate with weld fusion zone at right side; (b) view to right of (a) showing weld fusion zone and HAZ of 17.5 mm SPV490 reinforcement plate.



(a)



(b)

Figure 5-4. Microstructure of necked region at 106° location near EQH, sample SCV-106-2, 5×; (a) thinning deformation at base metal and weld HAZ in SPV490 alloy plate with weld fusion zone at right side; (b) view to right of (a) showing weld fusion zone and HAZ of 17.5 mm SPV490 reinforcement plate.

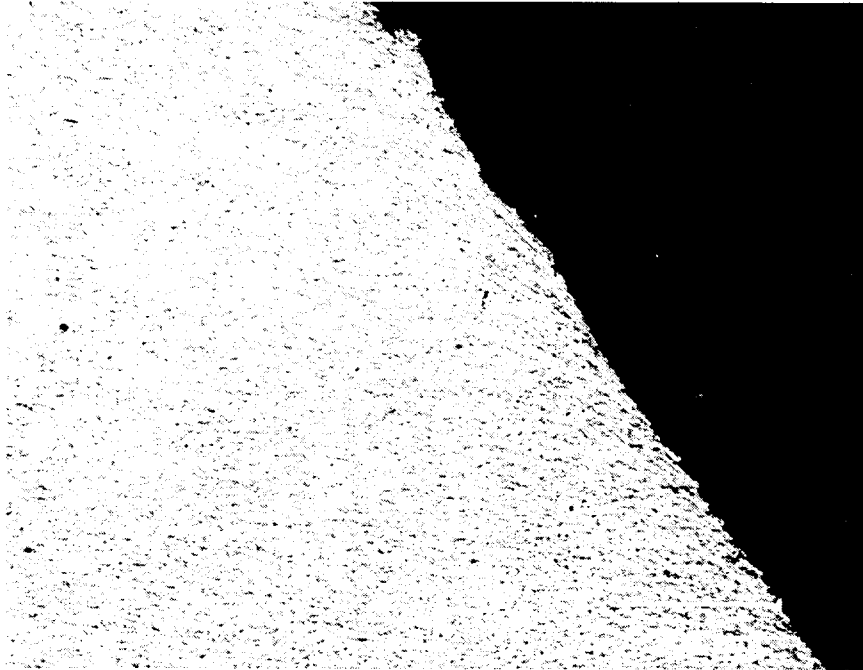


Figure 5-5. Local shearing associated in Sample SCV-74-2 with tearing near inner and outer surfaces near tear initiation site, and typical of the entire tear away from the initiation site, 100 \times .

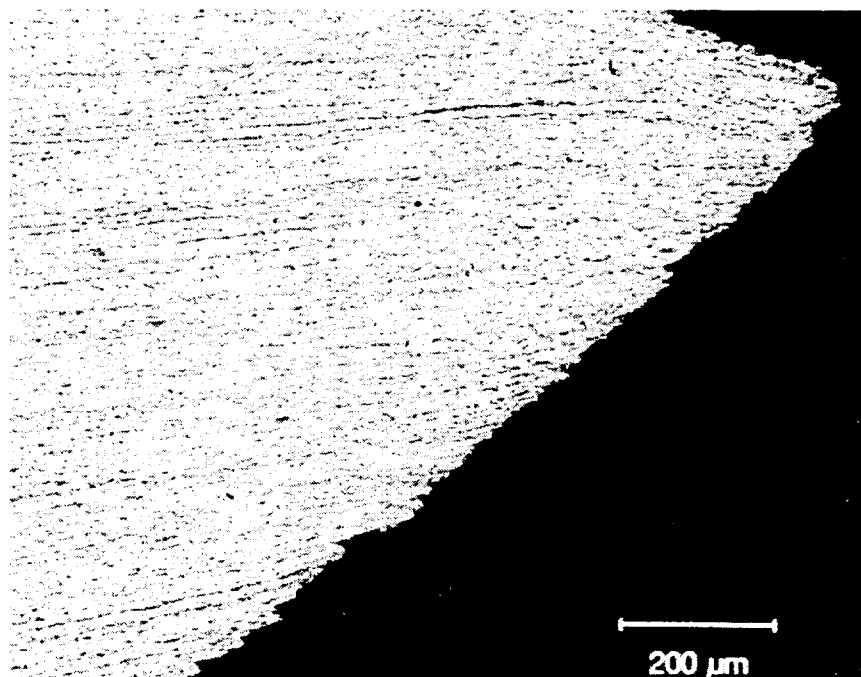


Figure 5-6. Relative absence of local shearing below the fracture surface in the interior of Sample SCV-74-2 denotes the actual fracture initiation site, 100 \times .

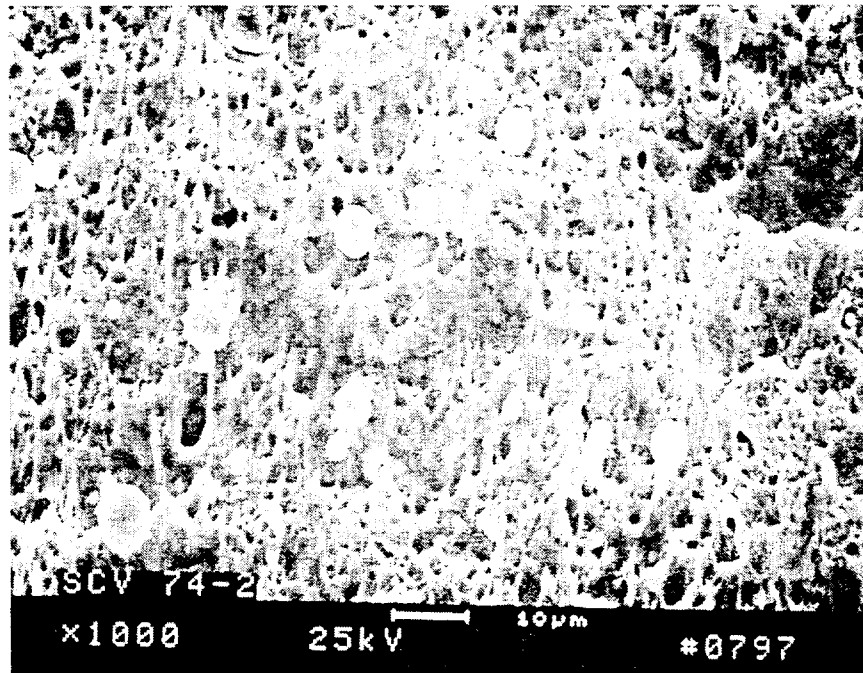


Figure 5-7. SEM image of ductile shear fracture on tear surface of SCV-74-2 sample taken from tear near EQH (round balls are surface contaminates on the sample).



Figure 5-8. Microstructure of Sample SCV-21. The neck in the vessel wall is located at the left side of the bottom of the hole in this view.

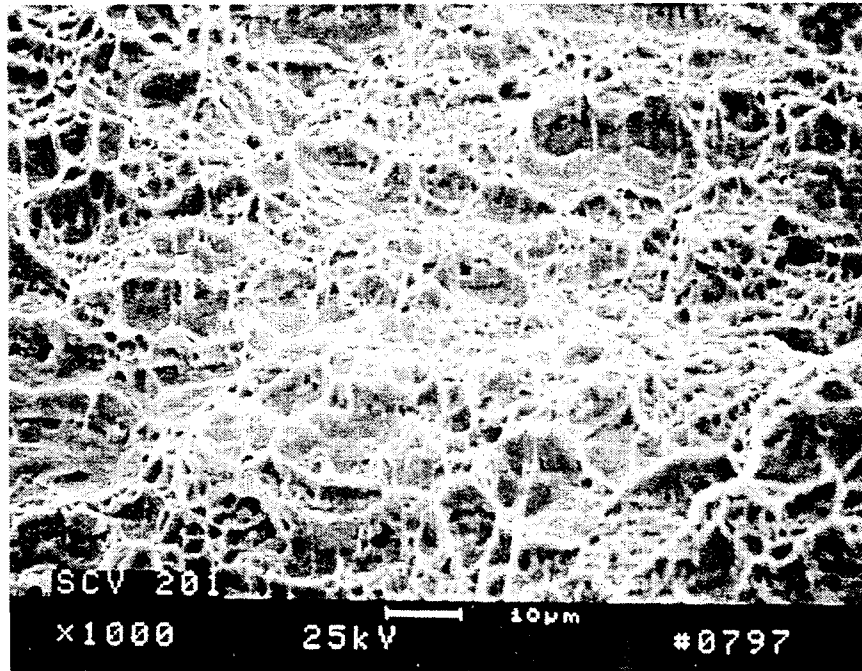


Figure 5-9. SEM image of ductile shear fracture on tear surface of SCV-201 sample taken from tear in wall below stiffener.

5.3 Samples from Deformed Vertical Weld Area

Sample SCV-340 consisted of two sections of 9 mm thick SPV490 welded vertically to one another. The microstructures and hardnesses of the fusion zone, heat affected zones, and base metal were similar to those described previously (Figure 5-10). Deformation was concentrated in the heat affected zones adjacent to each side of the weld, due to the low hardness in these regions. The reductions-in-area measured for each side of the weld are shown in Table 5-1.

6. Conclusions

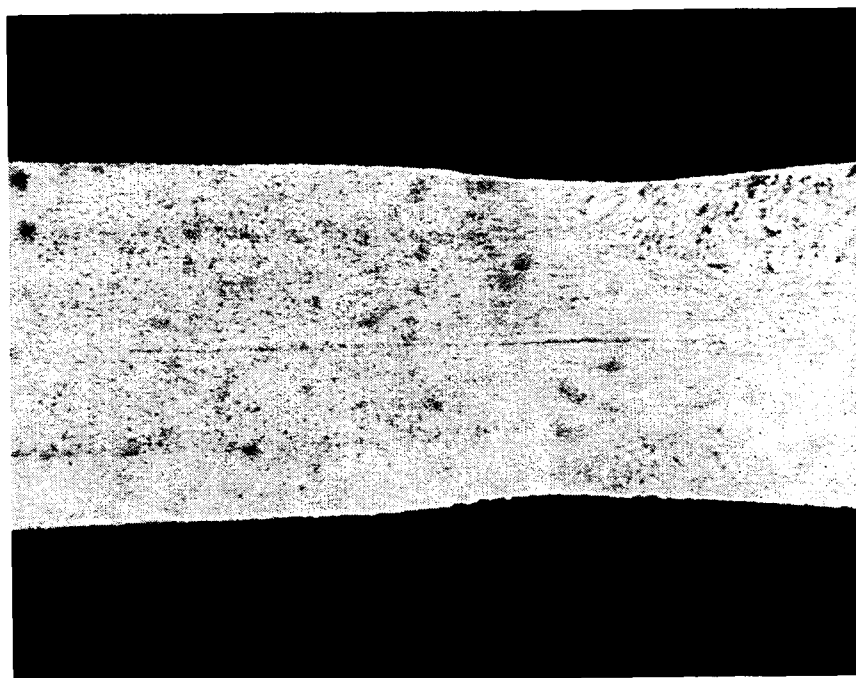
1. Strong local necking deformation occurred at two locations around the equipment hatch; at one, the 74° location, a large stable shear tear formed which caused a leak in the model. These deformations occurred preferentially in the weld heat affected region of the SPV490 plate.
2. Hardness measurements and metallographic analysis indicate that in the SCV model heat from the welding process resulted in localized microstructural alteration and reduced hardness and strength of the SPV490 alloy plate. The region of reduced hardness adjacent to the weld included the re-austenitized (dark etching) weld heat affected zone, 4 to 6 mm wide, and a narrow zone of reduced hardness HAZ, approximately 2 to 3 mm wide. The weld fusion zone was not significantly softer than the SPV490 base metal.

3. A second tear formed in the model wall, at a weld relief opening in a stiffener ring, at the 201° location where a vertical weld joined plates of SGV480 steel. A similar region at 21° formed a localized neck. These deformations also occurred within the weld heat affected region.
4. The microstructure and hardening mechanisms present in the SPV490 alloy make it sensitive to thermal history from the forming or welding process. The SGV480 alloy is less sensitive because of its simpler microstructure and chemistry.
5. All material deformation and fracture observed in the samples were ductile in nature. There was no evidence of material flaws, defects, or brittle behavior in the base metal or welds. The tears that occurred resulted from exceeding the local plastic ductility of the alloy. Measured fracture ductilities at the tear locations were consistent with the ductilities reported on the inspection certificates for the materials used to construct the model.

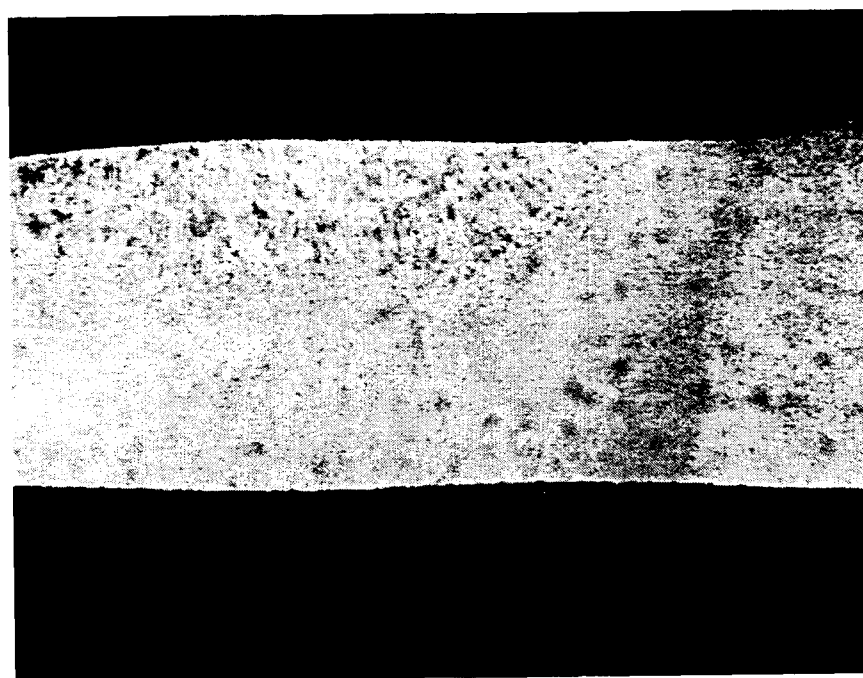
7. References

ASM Metals Handbook, 8th ed. 1967. pp. 1234–1236.

ASM Metals Handbook, 10th ed., Vol. 1. 1990. “High Strength Structural and High Strength Low Alloy Steels,” especially “Acicular ferrite/low-carbon bainite steels,” pp. 404–405.



(a)



(b)

Figure 5-10. Cross-section microstructure of vertical weld at 340° between plates of 9 mm SPV490 steel, Sample SCV-340; (a) plate material at left, necked HAZ at center, and weld fusion zone at right; (b) weld area to right of (a) showing, left to right, weld fusion zone, slightly necked HAZ, and 9 mm plate.

INTENTIONALLY LEFT BLANK

Appendix A

**Material Property Data and
Inspection Certificates**

INTENTIONALLY LEFT BLANK

Material property data

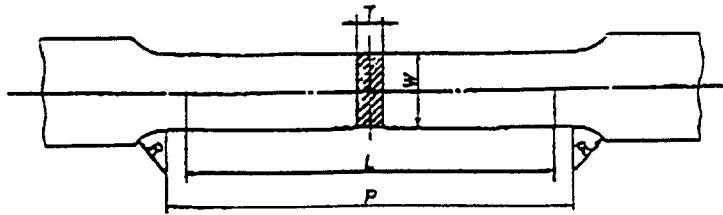
This is a response to Action Item NS-93-S-004. We received material property test results from the mill. Table-1 shows yield strength (yield point), tensile strength and elongation which were tested by the mill. The shape of the test specimens are shown in Figure-1 and 2. These specimens were taken transverse to the rolling direction of the plate.

If SNL has any question, please let me know.

Table-1 Material property data

Material	Thickness (mm)	Y. P.		T. S.		El. (%)	Ref. No.
		(kg/mm ²)	(N/mm ²)	(kg/mm ²)	(N/mm ²)		
SGV49 (SGV480)	6	39.2	384	58.0	568	22	SGV49-1
	7.5	41.1	403	58.7	556	28	SGV49-2
	8	39.7	389	54.3	532	26	SGV49-3
	8.5	41.9	411	57.1	560	24	SGV49-4
	10	41.4	406	57.3	562	24	SGV49-5
	38	37.4	366	54.0	529	31	SGV49-6
SPV50 (SPV490)	9	72.4	710	74.2	727	27	SPV50-1
	9	71.2	698	73.3	716	27	SPV50-2
	38	57.8	566	66.3	650	45	SPV50-3

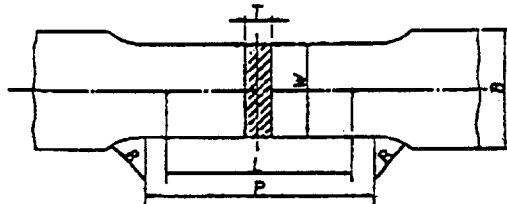
Y. P. : Yield Strength
T. S. : Tensile Strength
El. : Elongation



Unit: mm

Type of test piece	Width W	Gauge length L	Parallel length P	Radius of fillet R	Thickness T
1 A	40	200	approx. 220	25 min.	Thickness of material

Figure-1 Test specimen of SGV49



Unit: mm

Width W	Gauge length L	Parallel length P	Radius of fillet R	Thickness T
25	50	approx. 60	15 min.	Thickness of materials

Remark: In the case of applying this test piece to steel sheets not more than 3 mm thick, the radius R of fillet shall be 20 to 30 mm, and the width B of gripped ends shall be 30 mm or over.

Figure-2 Test specimen of SPV50

検査証明書
INSPECTION CERTIFICATE

說明書編號 : AURMC-796Z
 Classified No.

04 : 1993-03-29

0 H : 1993-03-29
036

Ship's No. _____

Construction No. : 088548

31 4 5 :AC1R549
Control No.

PW 02307

Surcouf's Order No 9102700

Yarlon Co. MARLBOROUGH CORPORATION

TRANSCENT CORPORATION.

Printed Doc No. : 0592 - DONIR549

Commodity HOT ROLLED STEEL PLATE

單 位 JIS 03118 5GV480 1987

Specification									
01	02	03	04	05	06	07	08	09	10



NIKK

日本興業株式会社
NKK CORPORATION

Specification

[illegible]

(7E) ☐ **PLATE ROLL** Indication of Plate Roll Number
(Notes) 15E: DM 1.2 letter the 1st 3 figures: mother Plate Number
17E: DM 1.4 the last 2 figures: divided Plate Number
☐ **DECEASED**

1	Job Position	NUMBER	Size of Impact Test Specimen
2	Time Test Was Run	1: 0x10mm 2: 7.5x10mm 3: 2.5x10mm 4: 5x10mm	
3	Time From Wt. Web	5: 1x10mm 6: 2.5x10mm 7: Thickness 10mm	
4	Impact Direction	NUMBER	Unit of Impact Test Property
5	L: Longitudinal	1: 144 - Energy 2: Char 3: Char. Mod. 4: J/Inch	
6	C: Transverse	5: U-Notch 6: Ft. Lbf	
7	Z: W. Through-thickness	Web Fracture: 8: Side Shear 9: Brittle	
8		10: Lateral Expansion 11: Min. 1 mil	

#5 Max M. George Lervach
 A: 20mm(=) O: 50mm(=)
 E: 50mm(=) H: 0(=)
 J: 2(=) K: 50(=)
 M: 5.65(=) P: 5.65(=)
 R: 40(=) S: 80mm(=)
 U: 100mm(=) Y: 2(=)

115-3-29 NO REC 66 3 24

上記商品は検査の結果判定の段階に合格していることを証明いたします。

(CAF70001) (RP902743)

野中旭, 吉田靖 沼根石井五郎
INSPECTOR TO

WE HEREBY CERTIFY THAT THE MATERIAL DESCRIBED HEREIN HAS BEEN TESTED AND INSPECTED WITH SATISFACTORY RESULTS IN ACCORDANCE WITH THE REQUIREMENTS OF THE ABOVE SPECIFICATION

京杭船政所：〒210 神奈川県川崎市川崎区南笹田町1番1号

KEIHIN WORKS: 1-1, MIYAMAWATARIDA-CHO, KAWASAKI 210 JAPAN

M. Tanaka
京浜製鉄所検査室長
Manager of Inspection

SGV49-2

検査証明書 INSPECTION CERTIFICATE



NKK 日本鋼管株式会社
NKK CORPORATION

本社：〒100 東京都千代田区丸の内1丁目1番2号
Head Office: 1-1-2, MARUNOUCHI, CHIYODA-KU, TOKYO 100 JAPAN

証明番号：AURNC-7965
Certificate No.

日付：1993-03-29
Date

品番：088551
Item No.

製造番号：AC1R555
Construction No.

契約番号：AC1R555
Contract No.

買主：HITACHI, LTD.-HITACHI

買主の注文番号：Purchaser's Order No.

注文番号：MARUENI CORPORATION

注文書番号：Reference No.

品名：HOT ROLLED STEEL PLATE

規格：JIS G3118 SV480 1987

仕様：SPECIFICATION

寸法：SIZE (MM)

重量：WEIGHT (KG)

化学成分：CHEMICAL COMPOSITION (%)

機械的性質：MECHANICAL PROPERTIES

引張試験：TENSILE TEST

圧延試験：FLAT TENSILE TEST

引張試験：TENSILE TEST

圧延試験：FLAT TENSILE TEST

引張試験：TENSILE TEST

圧延試験：FLAT TENSILE TEST

引張試験：TENSILE TEST

圧延試験：FLAT TENSILE TEST

引張試験：TENSILE TEST

圧延試験：FLAT TENSILE TEST

引張試験：TENSILE TEST

圧延試験：FLAT TENSILE TEST

引張試験：TENSILE TEST

圧延試験：FLAT TENSILE TEST

引張試験：TENSILE TEST

圧延試験：FLAT TENSILE TEST

引張試験：TENSILE TEST

圧延試験：FLAT TENSILE TEST

引張試験：TENSILE TEST

圧延試験：FLAT TENSILE TEST

引張試験：TENSILE TEST

圧延試験：FLAT TENSILE TEST

引張試験：TENSILE TEST

圧延試験：FLAT TENSILE TEST

引張試験：TENSILE TEST

圧延試験：FLAT TENSILE TEST

引張試験：TENSILE TEST

圧延試験：FLAT TENSILE TEST

引張試験：TENSILE TEST

圧延試験：FLAT TENSILE TEST

引張試験：TENSILE TEST

圧延試験：FLAT TENSILE TEST

引張試験：TENSILE TEST

圧延試験：FLAT TENSILE TEST

引張試験：TENSILE TEST

圧延試験：FLAT TENSILE TEST

引張試験：TENSILE TEST

圧延試験：FLAT TENSILE TEST

引張試験：TENSILE TEST

圧延試験：FLAT TENSILE TEST

引張試験：TENSILE TEST

圧延試験：FLAT TENSILE TEST

引張試験：TENSILE TEST

圧延試験：FLAT TENSILE TEST

引張試験：TENSILE TEST

圧延試験：FLAT TENSILE TEST

引張試験：TENSILE TEST

圧延試験：FLAT TENSILE TEST

A-6

(注) 1. 15桁の表示は、2桁の数字と1桁の数字の組合せで、母板番号を示す。
(Notes) 1. 15桁の表示は、2桁の数字と1桁の数字の組合せで、母板番号を示す。

2. 15桁の表示は、2桁の数字と1桁の数字の組合せで、母板番号を示す。
2. 15桁の表示は、2桁の数字と1桁の数字の組合せで、母板番号を示す。

3. 15桁の表示は、2桁の数字と1桁の数字の組合せで、母板番号を示す。
3. 15桁の表示は、2桁の数字と1桁の数字の組合せで、母板番号を示す。

検査者：M. Tanaka

検査日：1993.3.29

検査場所：〒210 神奈川県横浜市西区南横田町1番1号

検査結果：合格 (CAF71001) (RP4BZ743)

検査者：M. Tanaka

検査日：1993.3.29

検査場所：〒210 神奈川県横浜市西区南横田町1番1号

検査結果：合格 (CAF71001) (RP4BZ743)

検査場所：〒210 神奈川県横浜市西区南横田町1番1号 KEIHEI WORKS: 1-1, MINAMIWATARI 10A-CHO, KAWASAKI 210 JAPAN

M. Tanaka

SGV49-3

検査証明書
INSPECTION CERTIFICATE

本社：〒100東京都千代田区九の町1丁目1番2号
Head Office: 1-1-2, MARUNOUCHI, CHIYODA-KU, TOKYO 100 JAPAN

船名	: HITACHI, LTD.-HITACHI
船主	:
船務代理	: Nippon Yusen Kaisha Ltd.
船務代理	: MARUENI CORPORATION.
船務代理	: B292 -DGNR543
船務代理	: HOT ROLLED STEEL PLATE
船務代理	: JIS 0318 S0V480 SR 1967



NKK 日本興業株式会社
NKK CORPORATION

說明書番 号 :AURHC-7961
Date/CASE No.
日付
Date :1993-03-29
署名
Signature No. :
工 作 号
Construction No. :088547
封 鎖 番 号
Control No. :AC1R543

SPECIFICATION		Purchaser's Order No.		A. S. K. S.		Chemical Composition (%)		Tensile Test		Bend Test	
Roll No.	Heat No.	Size (MM)	Quantity	Mass (G)	C	Si	Mn	P	S	N	MM2
16024	YF89201	8 X 100 X 3000	283 KG	283.18	23	16	7	1		DC 389	532 26
VISUAL & DIMENSIONS : GOOD HEAT TREATMENT CONDITION FOR PLATE : 300 °C X 20 MIN. (A.C) (ROLL NO. YF892) HEAT TREATMENT CONDITION FOR TEST SPECIMEN : 820 °C X 1 HR. 30 MIN. STRESS RELIEVED (ITEM NO. 001)											
TENSILE TEST : Y. P. XMM T.S. ELONG. REDUCTION OF AREA 265 480 17 - 590 BENDIR = 1. DIRECTION AUSTENITE GRAIN SIZE : MXL 5 AUSTENITE GRAIN SIZE : 8.0											

(12) PLATE ROLL NO.
(Notes) 150: 00002 (letter the 1st 3 figures: mother Plate Number
172: 00004, the last 2 figures: divided Plate Number
02 00: 0012 Decoded

1. Test Position	5400442. Size of Impact Test Specimen
2. Test Tool F: 7799. Flange	1: 10x10mm 2: 5.10x10mm 3: 2.3x10mm 4: 5x10mm
3. Test Bottom W: 7.7. Web	5: 11x10mm 6: 5.2. 10x10mm 7: 2.1x10x10mm
4. Test Direction	10x10mm 11. Unit of Impact Test Property
5. Test Longitudinal	1244. Energy: 1. 10J. 2. 10J. 3. 10J. 4. 10J. 5. 10J.
6. Test Transverse	10J. 10J. 10J. 10J. 10J. 10J. 10J. 10J. 10J. 10J.
7. Test Through-thickness	10J. 10J. 10J. 10J. 10J. 10J. 10J. 10J. 10J. 10J.
8. Test Fracture	10J. 10J. 10J. 10J. 10J. 10J. 10J. 10J. 10J. 10J.
9. Test Shear	10J. 10J. 10J. 10J. 10J. 10J. 10J. 10J. 10J. 10J.
10. Test Brittle	10J. 10J. 10J. 10J. 10J. 10J. 10J. 10J. 10J. 10J.

1.5 MOTOR GAUGE Length
 A: 20mm (a) D: 50mm (a)
 E: 50mm (a) H: 8" (a)
 J: 2" (a) K: 50 (a)
 M: 3.85 (a) P: 5.85 (a)
 R: 4D (a) S: 60mm (a)
 U: 100mm (a) Y: 2" (a)

45-3-29 NUREC

45.3.29

上記商品が我が国の標準規格の規格に適合していることを証明いたします。

(CAF69002) (RP90Z743)

野中旭, 吉田 晴 明 佐井三郎
INSPECTOR TO

WE HEREBY CERTIFY THAT THE MATERIAL DESCRIBED HEREIN HAS BEEN TESTED AND INSPECTED WITH SATISFACTORY RESULTS IN ACCORDANCE WITH THE REQUIREMENTS OF THE ABOVE SPECIFICATION.

京張鐵路所：〒210 神奈川縣川崎市月島區月島町1番1号

KEIHIN WORKS; 1-1, MINAMIWATARIDA-CHO, KAWASAKI 210 JAPAN

M. Zanaka
京浜製鉄所検査
Manager of Inspection

SCV49-6

検査証明書 INSPECTION CERTIFICATE



本社 東京都千代田区丸の内1丁目1番2号
Head Office: 1-1-2, MARUNOUCHI, CHIYODA-KU, TOKYO 100 JAPAN

証明書番号 : AURHC-7963

Certificate No.

日付 : 1993-03-29

Date

品名

SPIN No. : 088549

Construction No.

契約番号 : AC1R550

Contract No.

買主 : HITACHI, LTD.-HITACHI.

買主番号

Purchaser's Order No. 99402700

注文書

Trading Co. : MARUBENI CORPORATION.

注文書番号

Reference No. : B592 -DGN1R550

品名

Commodity : HOT ROLLED STEEL PLATE

規格

JIS G3118 SGV480 1987

Specification

Roll No.	Purchaser's Order No.	Size (mm)	Quantity	Mass (kg)	Chemical Composition (%)						Tensile Test				IMPACT TEST			
											Y.P.	T.S.	E.L.	Y.R.	1	2	NOTCH	
SPECIFIED VALUE (STANDARD)											265	480	140	270	3	AVE	TEMP.	
(CUSTOMER'S SPEC.)																		
SN91301	001	38 X 1000 X 3000	1	29518	23	116	7	1			366	529	31	21.0	23.2	20.7	2MM V	EACH
16024															19.0	21.0	-25°C	
TOTAL				893KGS														
VISUAL & DIMENSIONS : GOOD																		
HEAT TREATMENT CONDITION FOR PLATE																		
NORMALIZED																		
900 °C X 60MIN. (A.C)																		
(ROLL NO. SN913)																		

(1) Indication of Plate Roll Number
(Notes) : 1. 56: 000. 2. Letterline 1st 3 figures: mother Plate Number
172: 000. the last 2 figures: divided Plate Number
(2) DG: 001. Debossed

1. Position
T: Top F: Front B: Bottom U: Under W: Web
2. Direction
L: Longitudinal
C: Transverse
Z: Through-thickness
3. Size of Impact Test Specimen
1: 10x10mm 2: 7.5x10mm 3: 2.5x10mm 4: 5x10mm
5: 1.5x10mm 6: 2.5x10mm 7: Thicknessx10mm
4. Unit of Impact Test Property
1: KJ/m² Energy: K: kJ/m², m: kJ/m², m: kJ/m², J: Joule.
U: UCV, F: Ft. Lbf
5. Fracture: S: Shear B: Brittle
6. Lateral Expansion: M: mm Limit
7. UT: 001. Dend Test
UT: 001. Ultrasonic Examination
Q: 001. G: 001

1. Gauge Length
A: 200mm(±) D: 50mm(±)
E: 50mm(±) H: 5(±)
J: 2(±) K: 150(±)
M: 5.65(±) P: 5.65(±)
R: 40(±) S: 50mm(±)
U: 100mm(±) V: 2(±)

NS-3-19 NUPEC 社, 9, 24

上記商品検査の結果指定の規格に合格していることを証明いたします。

(CAF71001) (RP4B2743)

野中 旭 検査 野中 研二郎
INSPECTOR TO

WE HEREBY CERTIFY THAT THE MATERIAL DESCRIBED HEREIN HAS BEEN TESTED
AND INSPECTED WITH SATISFACTORY RESULTS IN ACCORDANCE WITH THE
REQUIREMENTS OF THE ABOVE SPECIFICATION.

京浜製鉄所 〒210 神奈川県川崎市川崎区南郷田町1番1号 KEIHIN WORKS: 1-1, MINAMIWATARIDA-CHO, KAWASAKI 210 JAPAN

M. Tanaka
京浜製鉄所検査
Manager of Inspection

SPY50-1

検査証明書
INSPECTION CERTIFICATE

本社：〒100東京都千代田区丸の内1丁目1番2号
Head Office: 1-1-2, MARUNOUCHI, CHIYODA-KU, TOKYO 100 JAPAN

國 兵 軍 : HITACHI, LTD. - HITACHI

Purchaser's Order No 9402700

Trading Co., : MARUBENI CORPORATION.

Reference No. : B592 - DGNIR564

Commodity HOT ROLLED STEEL PLATE

JIS 03115 SPV490 Q 1990

星 明 密 指 号 : AURN-7969

Certificate No. _____

B N : 1993-03-29

DATE _____

Spine No. _____

Construction No. 1088639

:AC1R564

Contract No. _____

[illegible]

(7E) [] REMARKS: Indication of Plate Roll Number
 (Notes) : 1.5M:08A9.2 letter in the 1st 3 figures:mother Plate Number
 : 72H:08B6.9, the last 2 figures:divided Plate Number
 [] 03:081Z. Deceased

Ex. Position	INJ4442 Size of Impact Test Specimen
T:Top To F:Front, Flange	1:10x10mm 2:1.5x10mm 3:2:3x10mm 4:5x10mm
B:Back Bottom W:Web	5:1:3x10mm 6:2:5x10mm 7:Thicknessx10mm
RA Direction	INJ444244 Unit of Impact Test Property
1:Longitudinal	XXX- Energy: KJ of m. C:bf. m/cg. J:Joule.
C:Lat Transverse	U:/cg. P:ft. lbf
2:R Through-thickness	WFF- Fracture: S:SL Shear B:Br. Brittle

6. 200H. Gauge Length	
A: 200mm (w)	D: 60mm (w)
E: 50mm (e)	H: 8" (w)
J: 2" (e)	K: 60 (e)
M: 5. 65 (e)	P: 5. 65 (w)
R: 40 (e)	S: 80mm (w)
U: 100mm (w)	Y: 2" (w)

(H3) CE92=C+MN/6+SI/24+NI/40+CR/5+MO/4+V/14

HC-3-29 MURDO

229

上記商品は税関の届出税定の取扱いに各付していることを説明いたします。

1. ST: CIVIL BAND TEST
 2. UST: ~~ULTRASONIC~~ Ultrasonic Examination
 3. G: ~~ALL~~ GOOD

~~(CAF73001) (RPQB2743)~~

野牛池, 吉田清 明雄 研一郎 WE HEREDY CERTIFY, THAT THE MATERIAL DESCRIBED HEREIN HAS BEEN TESTED
INSPECTOR TO AND INSPECTED WITH SATISFACTORY RESULTS IN ACCORDANCE WITH THE
REQUIREMENTS OF THE ABOVE SPECIFICATION.

・京浜東北線：〒210 神奈川県川崎市川崎区南渡田町1番1号 KEIHIN WORKS:1-1, MINAMIWATARI-CHO, KAWASAKI 210 JAPAN

M. Tanaka
京浜製鉄所検査室

SPV50-2

検査証明書
INSPECTION CERTIFICATE



日本興業株式会社
NIKKO CORPORATION

本社：〒100東京都千代田区丸の内1丁目1番2号
Head Office: 1-1-2, MARUNOUCHI, CHIYODA-KU, TOKYO 100 JAPAN

證明書 番号 : AURNHC-7968
Certificate No.

日 14 : 1993-03-29

Ship's No. 1

CONSTRUCTION NO. : 080633

列 鈔 番 号 : AC1R558

Contract No. _____

圖・製 電 :HITACHI, LTD.-HITACHI

Purchaser's Order No 9402700

Trading Co., :MARUBENI CORPORATION.

REF ID: A6592 - DON1R558

Commodity HOT ROLLED STEEL PLATE

ALL INFORMATION CONTAINED HEREIN IS UNCLASSIFIED
DATE 03-11-15 BY SPV490 Q 1990

Specification

[illegible]

(E) ☐ ~~123456789~~ Indication of Plate Roll Number
(Notes) 1234: 1234, 2 letters the last 3 figures: mother Plate Number
1728: 1728, the last 2 figures: divided Plate Number
E2 ☐ 00: 00, Decoded

100. Position	200. Material	300. Size of Impact Test Specimen
110. Top Face	210. Alloy	310. 1x10x10mm 2: 7.6x10mm 3: 2x10mm 4: 5x10mm
120. Bottom Face	220. Heat Treatment	320. 5: 1x1x10mm 6: 2.5x10mm 7: Thickness 8: 10mm
130. Direction	230. Heat Treatment	330. Unit of Impact Test Property
140. Longitudinal	240. Heat Treatment	340. Energy: K: kgf. m. C: kgf. m/cm ² . J: joule.
150. Transverse	250. Heat Treatment	350. U: cal. F: ft. lb
160. Through-thickness	260. Heat Treatment	360. Fracture: S: 101. Shear B: 101. Brittle

Larval Measurements	
A: 2.00mm (u)	O: 5.0mm (u)
E: 9.0mm (u)	H: 8' (u)
J: 2' (u)	K: 5.0 (u)
M: 5.65 (u)	P: 5.65 (u)
R: 4.0 (u)	S: 8.0mm (u)
U: 1.00mm (u)	Y: 2' (u)

73 CF92=C+MN/6+SI/24+NI/90+CR/5+MO/4+V/14

NS-3-19 MWPTC

9.29

上記商品は数量の調整が可能な状態に合格していることを証明いたします。

野中松 吉田清 明雄 新田 明雄 WE HEREBY CERTIFY THAT THE MATERIAL DESCRIBED HEREIN HAS BEEN TESTED
AND INSPECTED WITH SATISFACTORY RESULTS IN ACCORDANCE WITH THE
REQUIREMENTS OF THE ABOVE SPECIFICATION.
INSPECTOR TO

・東横製鉄所：〒210 神奈川縣川崎市川崎區南横田町1番1号

KEIHIN WORKS: 1-1, MINAMIWATARIDA-CHO, KAWASAKI 210 JAPAN

M. Tanaka
京浜製鉄所検査所

SPV50-3

検査証明書
INSPECTION CERTIFICATE

本社：〒100東京都千代田区丸の内1丁目1番2号
Head Office: 1-1-2, MARUNOUCHI, CHIYODA-KU, TOKYO 100 JAPAN

商 標 註 冊 : HITACHI, LTD.-HITACHI

Purchaser
買家或客戶

Purchaser's Order No 9902700

匪文者

Trading Co. : MARUBENI CORPORATION.

在文初四角各需号
R#(R#R#R# R#

REFERENCE NO. : D592 - DGN1R557

Commodity **HOT ROLLED STEEL PLATE**

JIS 03115 SPV490 Q 1990

Special Collection

JIS 03115 SPV490 Q 1990

[illegible]

(7) ☐ Indication of Plate Roll Number

(Notes) 1256:EXH9.2 latter the 1st 3 flowers:mother Plate Number

2 DB: 2012, Doc

1	2	3	4	5	6	7	8	9	10	11	12	13	14	15	16	17	18	19	20	21	22	23	24	25	26	27	28	29	30	31	32	33	34	35	36	37	38	39	40	41	42	43	44	45	46	47	48	49	50	51	52	53	54	55	56	57	58	59	60	61	62	63	64	65	66	67	68	69	70	71	72	73	74	75	76	77	78	79	80	81	82	83	84	85	86	87	88	89	90	91	92	93	94	95	96	97	98	99	100
										NY Position																																																																																									

T: 4x1 Top F: 7979 Flange 1: 10x10mm 2: 7.5x10mm 3: 2/3x10mm 4: 5x10mm

B:PSL Bottom W:7.7 Web 5:1/3x10mm 6:2.5x10mm 7:Thickness 8x10mm

7. Unit of Impact Test Property

DATE: ENERGY: K: 101. M C: 101. HV: 101. J: 101. U: 101. E: 101. I: 101.

2:11 Through-thickness ~~WGT.~~ Fracture: 9:10, Shear 8:10, Brittle

Upper Lateral Expansion: Mmm 1mm

DOT : 21744 Bend Test

USY (1974a, b)
USY (1975)

5 NORTH GARDEN ROAD

A: 200mm(≡) D: 50mm(≡)

E: 50mm (•) H: 6" (•)

J:2' (•) X:5D(•)
1115 2571-1 015 2171

M:5.85A(●) P:5.85A(●)
R:0D(●) S:0D(●)

U: 100mm (寸) Y: 2" (寸)

[illegible]

CEQ2=C+MN/6+S1/24+NI/40+CR/5+MD/4+V/14

HS-1-29, NUPEC

41 7.79

上記商品は検査の基準指定の規格に合格していることを証明いたします

UST; ~~WJ222~~ Ultrasonic Examination

Dr. M. B. Gold

(CAF73001) (RP962743)

野中加吉 佐田 晴雄 佐田 晴雄
INSPECTOR TO WE HEREBY CERTIFY THAT THE MATERIAL DESCRIBED HEREIN HAS BEEN TESTED
AND INSPECTED WITH SATISFACTORY RESULTS IN ACCORDANCE WITH THE
REQUIREMENTS OF THE ABOVE SPECIFICATION.

東供創設所：〒210 神奈川県川崎市川崎区南浜田町1番1号

KEIHIN WORKS:1-1,MINAMIWATARIDA-CHO,KAWASAKI 210 JAPAN

M. Zanaka

INSPECTION CERTIFICATE

Heat No.	Material	Size (mm)			Chemical Composition (%)									Tensile Test (N/mm ²)		El (%)
		T	W	L	C	Si	Mn	P	S	Ni	Cr	Mo	V	Y.S	T.S	
TG86001	SGV480	6	×1000	×3000	0.18	0.26	1.14	0.006	0.001					384	568	22
SN91401	SGV480	7.5	×1500	×4000	0.18	0.23	1.16	0.007	0.001					403	556	26
TF89201	SGV480	8	×1500	×3000	0.18	0.23	1.16	0.007	0.001					389	532	26
SN91501	SGV480	8.5	×2500	×4500	0.18	0.23	1.16	0.007	0.001					411	560	24
SN91201	SGV480	10	×3000	×4500	0.18	0.23	1.16	0.007	0.001					406	562	24
SN91301	SGV480	38	×1000	×3000	0.18	0.23	1.16	0.007	0.001					366	529	31
TA91702	SPV490	9	×1500	×5000	0.10	0.24	1.29	0.002	0.001	0.48	0.03	0.17	0.04	710	727	27
TA91701	SPV490	9	×2500	×5000	0.10	0.24	1.29	0.002	0.001	0.48	0.03	0.17	0.04	698	718	27
TA91601	SPV490	38	×1000	×3000	0.10	0.24	1.29	0.002	0.001	0.48	0.03	0.17	0.04	566	650	45

T : Thickness
 W : Width
 L : Length

Y.S : Yield Stress
 T.S : Tensile Strength
 EL : Elongation

Appendix B

All Sample Hardness Measurements (Rockwell B Scale)

INTENTIONALLY LEFT BLANK

Listing of All Sample Hardness Measurements (Rockwell B scale)

Sample	Material	Zone Description	Average (x)	Std. Dev. (s)	Raw Data									
Plate	SPV490	Reference Plate	98.8	0.7	99.2	98.1	97.6	98.4	98.6	100.1	98.5	99.2	99.0	98.8
SCV-74-1	SPV490	Base Metal	98.1	1.0	98.8	99.6	98.4	98.7	98.0	96.5	96.3	99.1	98.5	97.4
		HAZ	91.5	1.1	92.8	92.1	90.1	90.4	92.1					
		Fusion Zone	95.1	1.1	95.5	94.7	96.4	95.6	93.3					
SCV-74-3	SGV480 (Side)	Base Metal	89.18	0.15	89.0	89.1	89.3	89.1	89.4					
		HAZ	92.20	1.49	89.9	94.3	91.4	92.3	93.1					
	SPV490 (Side)	Base Metal	94.24	0.39	94.8	94.4	93.9	93.7	94.4					
		HAZ	90.82	1.80	90.1	89.3	89.2	92.2	93.8					
		Fusion Zone	92.10	0.96	92.7	90.2	92.6	92.7	92.3					
SCV-106-1	SPV490	Base Metal	97.36	1.22	97.4	98.6	97.2	99.0	97.2	96.6	96.2	97.5	96.6	96.4
					97.1	96.2	95.5	97.2	100.0	97.6	96.5	96.5	98.0	100.3
		HAZ	92.06	1.69	95.1	92.7	91.0	91.0	90.5					
		Fusion Zone	97.21	1.11	98.6	98.6	97.8	97.3	98.4	96.3	95.5	95.8	95.9	96.7
					97.6	98.4	96.2	98.6	96.4					
SCV-106-2	SPV490	Base Metal	96.96	1.34	94.8	95.4	95.3	96.4	99.8	97.4	98.6	97.2	99.0	97.2
					96.6	96.2	96.5	96.6	96.4					
		HAZ	88.64	1.04	90.1	89.5	87.3	87.8	88.5					
		Fusion Zone	94.93	2.58	94.1	94.7	96.5	98.3	98.9	91.7	90.6	92.7	96.1	95.8
SCV-340	SPV490	Base Metal	97.93	0.84	96.8	99.1	99.0	96.5	96.8	98.3	98.5	98.7	98.3	98.4
					98.3	98.3	97.9	98.1	98.5	96.8	97.9	96.2	97.5	98.7
		HAZ	96.65	1.83	93.8	97.0	97.5	98.3	92.9	98.4	98.1	97.7	97.2	95.6
		(areas of minimum deformation)												
		Fusion Zone	97.63	0.55	97.1	97.7	98.1	97.2	96.4	97.3	97.6	98.4	97.8	98.1
SCV-21	SGV480				98.6	97.4	97.8	97.7	97.2					
		Base Metal	88.82	1.26	89.7	90.3	90.0	88.4	87.3	87.2				
		HAZ	92.75	0.56	92.6	92.4	92.3	93.7						
		(undeformed area)												
		HAZ	95.08	2.27	91.0	94.7	95.3	97.1	97.3					
		(deformed area)												
		Fusion Zone	95.53	0.82	95.9	94.6	95.7	97.3	94.7	95.0				

INTENTIONALLY LEFT BLANK

Distribution:

Nuclear Power Engineering Corporation
Attn: Satoru Shibata (14 copies)
Systems Safety Department
Fujita Kanko Toranomon Bldg. 5F
17-1, 3-Chome Toranomon, Minato-ku
Tokyo, 105
Japan

U. S. Nuclear Regulatory Commission
Attn: James F. Costello
Division of Engineering Technology
Structural and Geological Engineering Branch
TWFN/MS T-10L1
Washington, DC 20555-0001

University of Tokyo
Attn: Prof. Genki Yagawa
Dept. of Quantum Engineering and System
Science
7-3-1, Hongo, Bunkyo-ku,
Tokyo, 113
Japan

Kyushu University
Attn: Prof. Noriyuki Miyazaki
Chemical Engineering Group
Dept. of Materials Process Engineering
Graduate School of Engineering
6-10-1 Hakozaki, Higashi-ku
Fukuoka, 812-81
Japan

Argonne National Laboratory
Attn: Phillip Pfeiffer
Ronald Kulak
Computational Mechanics Section
9700 South Cass Ave.
RE, Bldg. 208
Argonne, IL 60439-4842

Agenzia Nazionale per la Protezione
dell'Ambiente (ANPA)
Attn: Giovanni Pino
Giuseppe Maresca
Via Vitaliano Brancati, 48
00144 Rome
Italy

General Dynamics Electric Boat Division
Attn: Kenneth Arpin
Amy Beacham
Nuclear Engineering, Department 470
75 Eastern Point Road
Groton, CT 06340-4989

Japan Atomic Energy Research Institute (JAERI)
Attn: Kazuichiro Hashimoto
Severe Accident Research Laboratory
Tokai-mura
Ibaraki-ken, 311-1195
Japan

Mitsubishi Research Institute, Inc.
Attn: Kenji Niiyama
Otemachi 2-3-6
Chiyoda-ku
Tokyo, 100-8141
Japan

Universität Stuttgart (MPA)
Attn: Ludwig Stumpfrock
Staatliche Materialprüfungsanstalt
Pfaffenwaldring 32
D-70569 Stuttgart (Vaihingen)
Germany

Thomas Ahl
14417 Country Club Lane
Orland Park, IL 60467

ABB Combustion Engineering, Inc.
Attn: Lyle D. Gerdes
Nuclear Power Division
2000 Day Hill Road
P. O. Box 500
Windsor, CT 06095-0500

TJBG Consulting Inc
Attn: Theodore E. Johnson
1435 Waters Edge Dr.
Augusta, GA 30901

Westinghouse Electric Corp
Attn: Richard S. Orr
Nuclear & Advanced Technical Division
MS 3-05
P. O. Box 355
Pittsburgh, PA 15230-0355

Purdue University
Attn: Prof. Mete A. Sozen
Kettlehut Distinguished Professor
School of Civil Engineering
1284 Civil Engineering
West Lafayette, IN 47907-1284

Stevenson & Associates
Attn: John D. Stevenson
9217 Midwest Avenue
Cleveland, OH 44125

Electric Power Research Institute (EPRI)
Attn: H. T. Tang
3412 Hillview Avenue
P. O. Box 10412
Palo Alto, CA 94303

General Electric Co.
Attn: Harold Townsend
ABWR Programs
175 Curtner Avenue
M/C-780
San Jose, CA 95125

NPS Energy Service
Attn: Joseph J. Ucciferro
Day & Zimmerman International, Inc.
President, Field Operations Division
1818 Market Street
Philadelphia, PA 19103-3638

Walter A. von Riesemann
7928 Woodhaven Drive NE
Albuquerque, NM 87109-5261

Cornell University
Attn: Prof. Richard N. White
School of Civil & Environmental Engineering
Hollister Hall
Ithaca, NY 14853

ANATECH Corporation
Attn: Yusef R. Rashid
Robert A. Dameron
5435 Oberlin Drive
San Diego, CA 92121

Internal:

MS 0342	R. P. Goehner, 1822
MS 0342	K. H. Eckelmeyer, 1822 (5 copies)
MS 0443	H. S. Morgan, 9117
MS 0443	S. W. Key, 9117
MS 0443	V. L. Porter, 9117
MS 0736	T. Blejwas, 6400
MS 0742	J. Guth, 6414
MS 0744	D. L. Berry, 6403
MS 0744	J. L. Cherry, 6403
MS 0744	M. F. Hessheimer, 6403
MS 0744	E. W. Klammer, 6403
MS 0744	V. K. Luk, 6403 (20 copies)
MS 0744	M. S. Luker, 6403
MS 0744	G. S. Rightley, 6403
MS 0744	J. A. Smith, 6403
MS 0748	J. S. Ludwigsen, 6413
MS 0783	D. W. Pace, 5854
MS 1134	J. A. Van Den Avyle, 1835 (5 copies)
MS 1407	R. J. Salzbrenner, 1835
MS 9018	Central Technical Files, 8940-2
MS 0899	Technical Library, 4916 (5 copies)
MS 0612	Review and Approval Desk, 4912 For DOE/OSTI (2 copies)